Table 1. The Results of aCGH Analysis of the Length of the Gene-Deleted Region and Disease Genes.

Patient	Sex	Deletion gene	Genotype (UCSC hg17 May 2004)	aCGH Deletions size (kb)	mother
1	M	*CYBB*	chrX:g.(37367763_37367821)_(37426362_37426421) del	58.7	carrier
2	M	*CYBB, DYNLT3*	chrX:g.(37402945_37403004)_(37487331_37487390) del	84.4	carrier
			chrX:g.(37514480_37514539)_(37606312_37606370) dup	91.9	
3	M	*XK, CYBB, DYNLT3*	chrX:g.(37128233_37128292)_(37722014_37722073) del	593.8	carrier
4	M	*XK, CYBB, DYNLT3*	chrX:g.(35599031_35599090)_(37543467_37543526) del	1944.5	-
5	F	*DMD, XK, CYBB, DYNLT3*	chrX:g.(32167387_32167446)_(37878746_37878805) del	5711.4	carrier

CYBB, cytochrome b-245, beta polypeptide; XK, X-linked Kx bood group gene; DMD, Duchenne muscular dystrophy gene; DYNLT3, dynein, light chain, Tctex-type3.
doi:10.1371/journal.pone.0027782.t001

the telomere side in patient 2 was shown by DNA walking analysis to be chrX:g.37398670 in intron 2 of the *CYBB* gene (Figure 3). The base sequence detected at the breakpoint was 5′-AGGTAT|GT-GAGCTGCCAC---- 3′ (| denotes the breakpoint). A search using NCBI Blast Human Sequences showed that this base sequence corresponded to a sequence inversion observed from chrX:g. 37612397 on the telomere side of the complementary strand. On the other hand, a search in the neighborhood of chrX:g.37612392, thought to be the breakpoint on the centromere side, found the normal 5′-GTGGCAGCTCAC|ATACCTAATCTGGACAG-C----3′ chromosomal base sequence. Because of this, it is thought that a 91.9 kb base sequence duplication as well as the deletion of an 84.4 kb base sequence shown by the results including aCGH analysis occurred in patient 3, and that since the duplicate centromere side end had the sequence 5′-AGGTAT-3′ on the complementary strand, one of the duplicate strands must have inverted and recombined with the common 5′-AGGTAT-3′ sequence at the telomere side of the 5′ breakpoint of the 84.4 kb deletion. However, although the base sequence of the binding region thought to be present between the duplicate strands was investigated by the step-by-step PCR method and DNA walking analysis, it is as yet unclear.

Investigation of skewed lyonization by methylation specific PCR

The analysis was conducted using peripheral blood mononuclear cells (PBMCs) from patient 5 and her mother. An abnormal (with deletion) X-chromosome from the mother (X1: 186 bp allele) and a normal X-chromosome from the father (X2: 195 bp allele) had been inherited. In the patient, a markedly skewed inactivation pattern was observed in which X-chromosomes from which genes had been deleted were activated and X-chromosomes with normal gene alleles were inactivated (Figure 6).

Discussion

The aCGH analysis showed gene deletions of various sizes ranging from 58.7 kb to 5.71 Mb. In patient 1, only the *CYBB* gene was deleted, whereas CGS associated with simultaneous deletions of adjacent genes occurred in the other patients.

In patients 1 and 2, precise breakpoints were analyzed by direct sequencing methods after amplification with PCR and DNA walking. Analysis of four patients including two patients[4] previously reported by us found two cases in which all genes within the breakpoints were deleted and one case each of complex

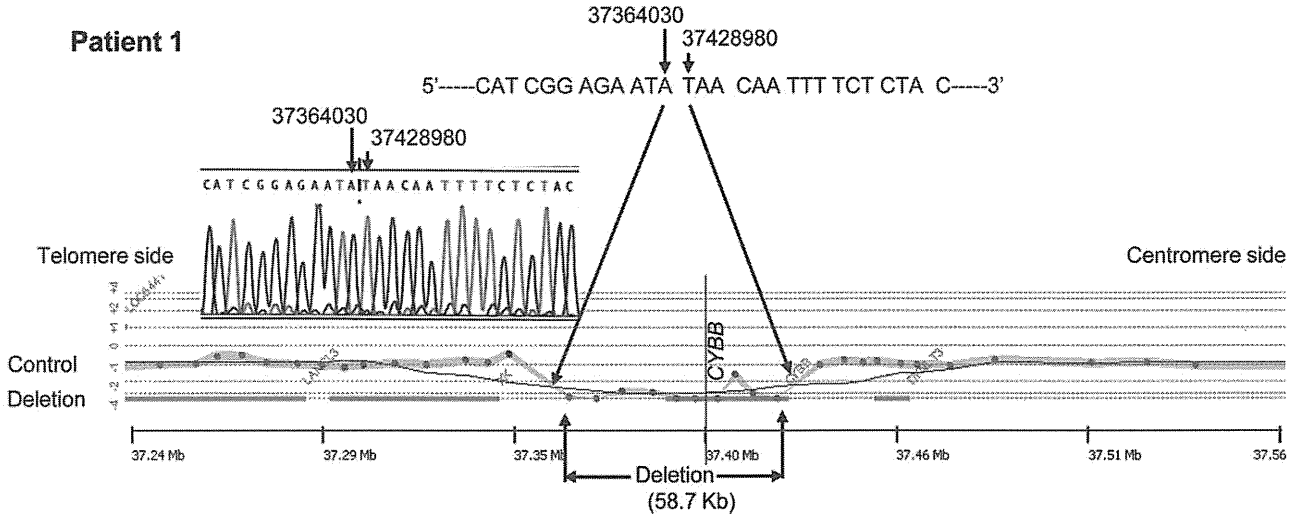

Figure 2. The Results of aCGH and Direct Sequence Analysis Spanning the Deletion Breakpoints in Patient 1. A female's DNA was used for the control DNA. aCGH analysis showed the deletion region to be 58.7 kb and direct sequencing after amplification by PCR showed that genes had been deleted from 37364030 to 37428980 (UCSC hg17 May.2004) and both breakpoints were bound.
doi:10.1371/journal.pone.0027782.g002

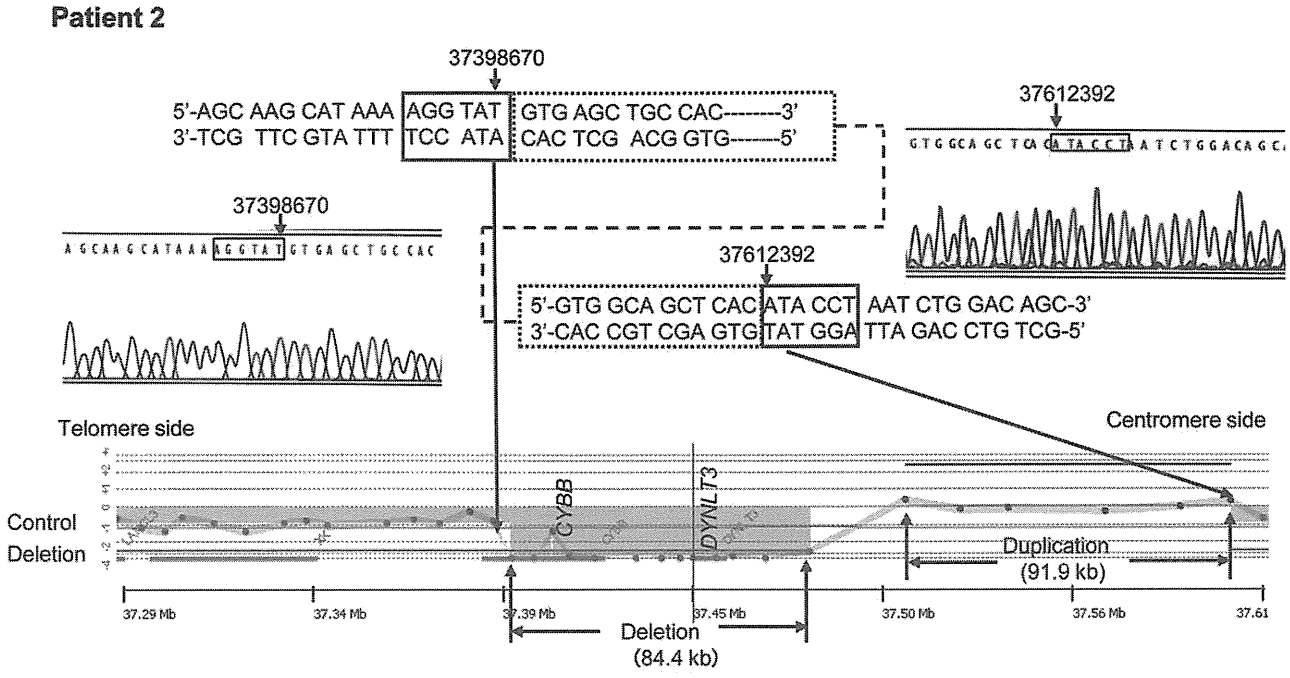

Figure 3. The Results of aCGH and Direct Sequence Analysis Spanning the Deletion Breakpoints in Patient 2. A female's DNA was used for the control. According to aCGH, the deletion site was 84.4 kbp and the duplication site 91.9 kb. According to the DNA walking analysis by PCR, a breakpoint was located at 37398670 of *CYBB* intron 2. Furthermore, six bases of the gene at 37612392 (UCSC hg17 May.2004) of ATACCT were bound inverted at the breakpoint, and complex structural abnormalities showing gene deletions on the inner side and duplication of the inverted part were observed.
doi:10.1371/journal.pone.0027782.g003

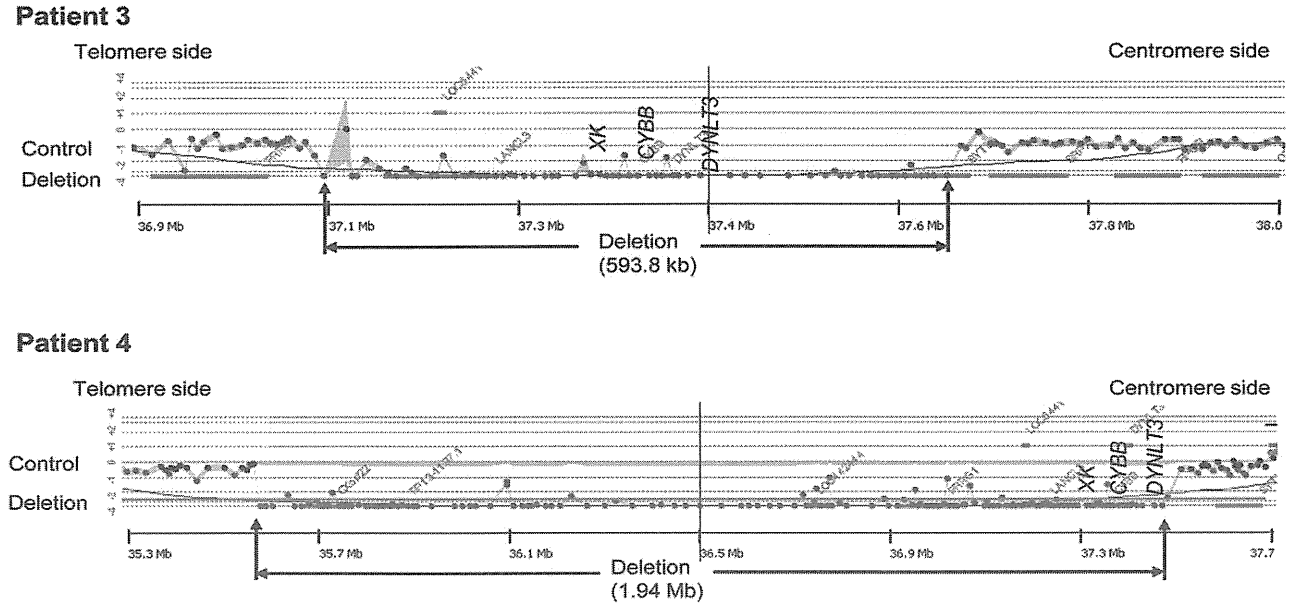

Figure 4. The Results of aCGH Analysis Spanning the Deletion Breakpoints in Patients 3 and 4. A female's DNA was used for the control DNA for patient 3, and a male's for patient 4. These male infants suffered deletions of three genes: the chronic granulomatous disease gene (*CYBB*), the McLeod syndrome gene (*XK*), and *DYNLT3*. The gene deletions in each patient were found to be 0.59 Mb and 1.94 Mb, respectively.
doi:10.1371/journal.pone.0027782.g004

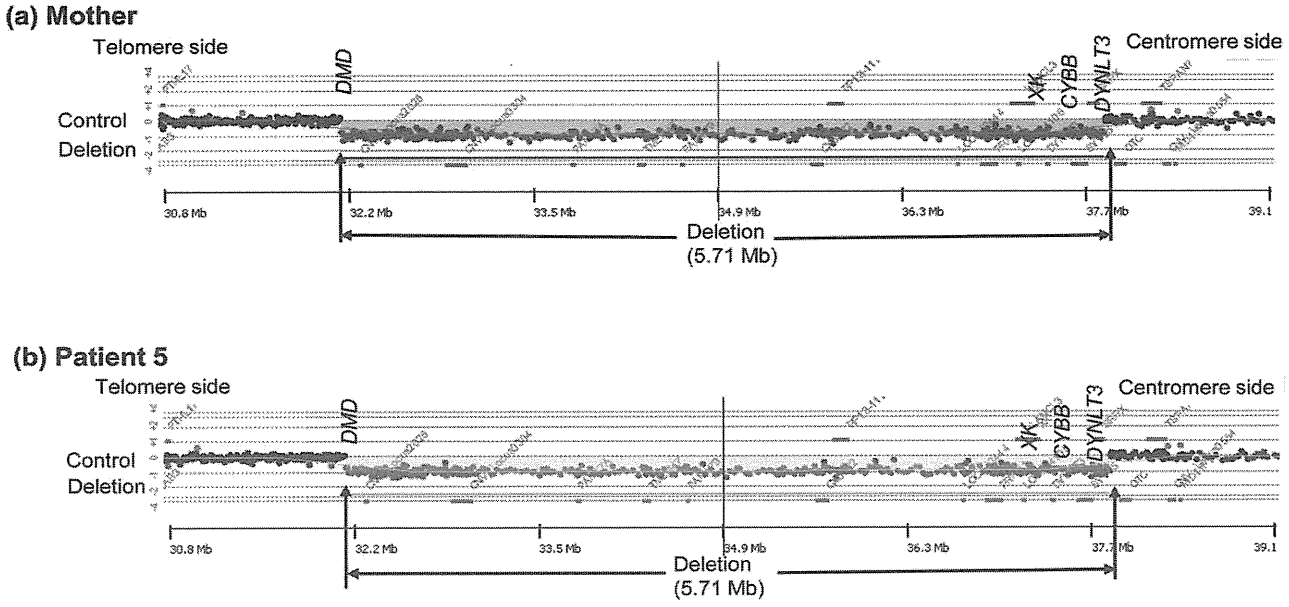

Figure 5. The Results of aCGH Analysis Spanning the Deletion Breakpoints in Mother and Patient 5. A female's DNA was used for the control DNA. This case involved deletions of four genes, the chronic granulomatous disease gene (*CYBB*), the Duchenne muscular dystrophy gene (*DMD*), the McLeod syndrome gene (*XK*), and *DYNLT3*. The gene deletion region was about 5.71 Mb and encompassed an area from *CYBB* to the greater part of the *DMD* (b). A similar gene deletion was also observed in the mother (a).
doi:10.1371/journal.pone.0027782.g005

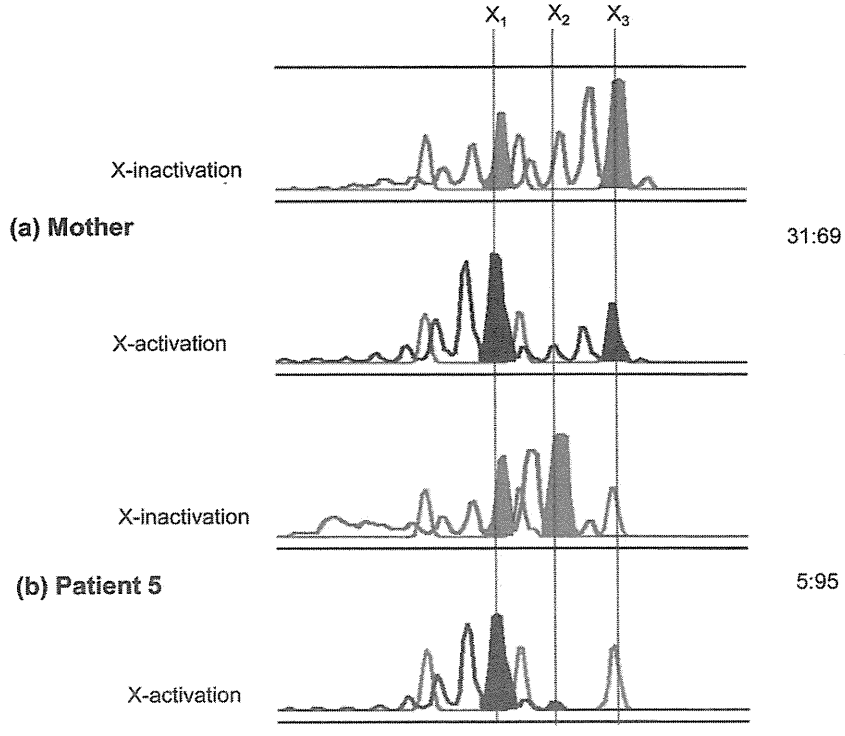

Figure 6. The Results of an Analysis of X-Chromosome Inactivation and Activation Patterns in the Chronic Granulomatous Disease Sufferer Patient 5 and Her Mother. The female infant had inherited an abnormal (with deletion) X-chromosome X1 from the mother and a normal X-chromosome X2 from the father. A random inactivation pattern of 69:31 was observed in the mother (carrier). In the female patient, however, a markedly skewed X-chromosome inactivation pattern of 95:5 (with activation of the X-chromosome with gene deletions transmitted from the mother and inactivation of the X-chromosome with the normal genes transmitted from the father) was observed.
doi:10.1371/journal.pone.0027782.g006

structural abnormalities associated with gene insertions and further inversions in addition to deletions. The ends in four patients had no gene sequences expected to result in a common breakpoint.

Chromosomal deletions require a search over the entire range since variation in extent may produce false negatives by PCR and duplication of other regions may be involved. Conventionally, chromosome banding and fluorescence in situ hybridization (FISH) [7–9] have been used for analysis of chromosomal deletions, duplications, and translocations, but with chromosome banding, the detection limit is 1 Mb or more even in analyses with well-resolved prometaphase chromosomes. On the other hand, a combination of PCR and automated fluorescent DNA sequencing allows analysis of single base mutations on the chromosome and offers the highest resolution. However, the length of the deletion varies depending on the patient and for larger deletions, it is difficult to set primers. In addition, when no PCR products are generated, it is thought that nucleotide insertion into the deletion site or mutations in the base sequence at the primer binding site may have occurred. In recent years, aCGH has been developed and come into use as a method of analyzing CNVs on chromosomes. In principle, aCGH is a method of adhering a human gene-specific oligonucleotide probe to a glass slide and competitively hybridizing it with patient and control DNA, each labeled with different fluorochromes, and detecting deletions in the genome and amplification at a resolution of several kb by measuring the fluorescence. But while this method has high specificity and high resolution, it has the disadvantage including difficulty in identifying chromosomal translocations.

Deletions due to genomic mutations are often caused by tandem repeats and interspersed repeats. Interspersed repeats in particular include shorts direct repeats, interspersed repeat elements (e.g. Alu repeats), inverted repeats, low copy number long repeats, and active transposable elements and are prone to large scale deletions and duplications [10,11]. In patient 1, the entire *CYBB* gene within the breakpoints was deleted. The *CYBB* gene in patient 2 was found up to exon 2 and entirely deleted from exon 3. Moreover, it displayed a complex structure in which the breakpoint chrX:g.37398670 bound to the base sequence inverted from 37612392 and the region downstream of 37612392 (UCSC hg17 May. 2004) exhibited a successive existing base sequence. Alu sequences, which existed the most, were observed in the neighborhood of the ends, but were not directly involved in the breakpoints.

Patient 5 was female but was diagnosed with CGD, having a history of increased susceptibility to infection and confirmed as 46, X del (X) (p 21.1 p.21.2) on chromosome banding. aCGH showed that the mother was a carrier with an X-chromosome with the same deletion as the patient. The existence of skewed lyonization was investigated by analysis of X-chromosome inactivation on the basis of DNA methylation [12]. In the analysis of the patient and her mother, she had inherited an abnormal X-chromosome (X1: 186 bp allele) from her mother and a normal X-chromosome (X2: 195 bp allele) from her father. A markedly skewed inactivation pattern was observed in the patient, where the X-chromosome with deleted genes was activated and the X-chromosome having the normal genetic allele was inactivated (Fig. 6). In consideration of these results and of the measured percentage of gp91-positive cells in the patient's neutrophils (markedly low at about 5%) in addition to the notably decreased ability to produce ROS when measured by the NBT assay (as described later in the "Materials and Methods" section), the normal X-chromosome was thought to be inactivated in the majority of cells of this patient, which was believed to be a factor at the onset of the disease (a symptomatic carrier). Each cell expresses alleles from only one X-chromosome. Reports on skewed lyonization include Bruton tyrosine kinase (BTK) deficiency (OMIM 300300) [13], DMD [14] and CGD [15–17], however, CGS associated with deletions to the same wide extent as in this patient has not been observed. Francke et al. [18] reported the case of a male infant in which CGD with extensive X-chromosome deletions was complicated by DMD, retinitis pigmentosa, and mental retardation. Here, we analyzed the case of a female infant who exhibited a similar phenotype with an extensive genomic deletion and revealed that the X-linked recessive disorder of women was caused by skewed lyonization.

While chromosomal deletions, inversions, and duplications occur singly or in combination, reciprocal recombinations due to translocations have been reported [19–21]. In patient 1, it was speculated that gene rearrangements due to non-homologous end-joining (NHEJ) showing the repeated sequence of only two bases (TA) at the ends of the deleted gene may have occurred (Figure 7.1a, 1b). Patient 2 had a complex structural abnormality, and it was hypothesized that this may have been caused by fork stalling and template switching (FoSTeS)/microhomology-mediated break-induced replication (MMBIR) [22,23]. In patient 2, a three base repeat sequence of AAT prone to cause changes in copy number or sequence swaps was observed in the original DNA strand that acts as a template for the lagging strand during DNA replication. This AAT is thought to bind to a complementary DNA sequence of TTA nearby on the same strand of DNA, forming a loop and inhibiting expansion of the replication fork (Figure 7.2a). Furthermore, releasing the leading strand with the free 3′ end, AGGTAT, and binding to the complementary strand ATACCT of another replication fork, a leading strand 5′-AGGTATGTGAGC----3′ was synthesized (Figure 7.2b). The gene synthesized on the leading strand is hypothesized to cause structural abnormalities leading to duplications and inversions of the DNA strand subsequent to the deleted DNA strand by a return to the lagging strand after the end of replication and the binding of the 5′---- GCTCACATACCT-3′ telomere side terminus with the normal gene to the 5′-AGGTATGTGAGC----3′ centromere side terminus gene by DNA ligase (Figure 7.2c). As far as we could find, while a breakage-fusion-bridge cycle has been reported as a mechanism for large structural abnormalities causing deletions, inversions, and duplications during chromosome division [23], no cases of structural abnormalities occurring in the vicinity of the same gene have been observed.

Materials and Methods

Subjects

The subjects were five Japanese X-linked CGD patients estimated to have large base deletions of 1 kb or more in the *CYBB* gene (four male patients, one female patient) and the mothers of four of these patients. The four male patients were diagnosed as CGD on the basis of the past history with increased susceptibility to infection, and of deficiencies in ROS productivity by the nitroblue tetrazolium test (NBT) and the neutrophil chemiluminescence method. Two of the male patients exhibited reduced expression of erythrocyte Kell blood group antigen, acanthocytosis, and also high serum CPK activity. In the female infant patient, in addition to a history of increased susceptibility to infection at the age of 11 and a marked reduction in ROS productivity to around 5% of normal, chromosome banding showed 46, X, del (X)(p21.1p21.2), and CGD was clinically diagnosed.

DNA isolation

All the patient samples in the present study were used with the approval of the Saitama Children's Medical Center Ethics

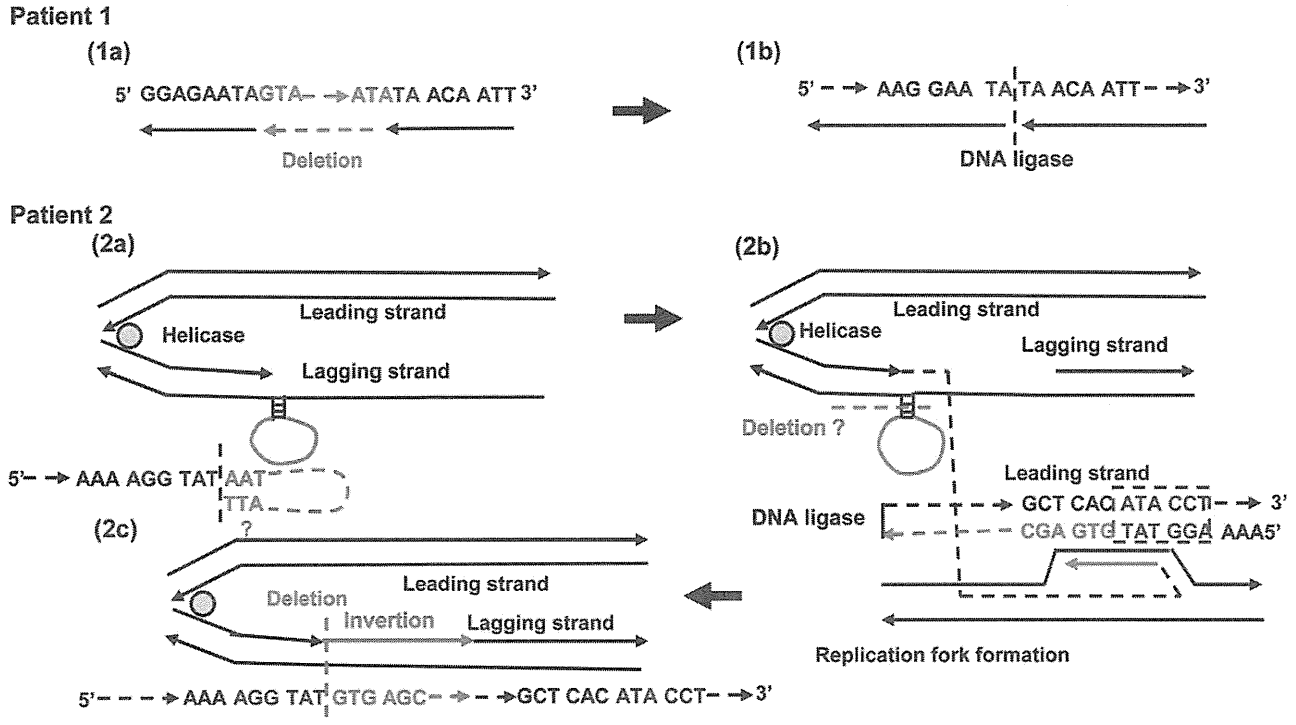

Figure 7. Genomic Rearrangement Mechanisms. For the gene deletions in patient 1, gene rearrangements exhibiting deletions due to non-homologous end-joining (NHEJ) were thought to have occurred, since repeated two base sequences of TA were observed at both ends of the gene (1a, 1b). In patient 2, it was hypothesized that rearrangement might have occurred through a mechanism involving a combination of fork stalling and template switching (FoSTeS)/microhomology-mediated break-induced replication (MMBIR). A three base repeat sequence of AAT prone to cause changes in copy number or sequence swaps was observed in a discontinuous end of the lagging strand during DNA replication. This formed a loop by binding to TTA on its complementary strand with replication slippage occurring (2a). At the discontinuous end, the lagging strand with the loop formed had a six base microhomology of AGGTAT and dissociated. The dissociated end subsequently bound to the ATACCT found at the duplication front of the leading strand. Synthesis and extension of the leading strand then occurred originating from the binding site (2b). The gene synthesized on the leading strand is hypothesized to cause structural abnormalities leading to duplications of the DNA strand subsequent to the DNA strand deletion by returning to the lagging strand after the end of duplication and the binding of the end that has finished duplication to the starting end of the normal gene on the lagging strand by DNA ligase (2c).
doi:10.1371/journal.pone.0027782.g007

Committee and after obtaining written informed consent, and the procedures were conducted to the principles expressed in the Declaration of Helsinki, 2008. Patient's parents provided written informed consent. DNA was extracted with a DNA Blood Mini Kit (Qiagen, Valencia, CA) after isolation of heparinized PBMCs.

PCR-band studies

CYBB gene and the adjacent X-linked Kx blood group-related *XK* gene were amplified by PCR and the detection of individual genes was attempted using the Agilent 2100 Bioanalyzer (Agilent Technologies, Santa Clara, CA) according to the manufacturer's instructions. The following primers were used for PCR: *CYBB* ex1: forward, 5′-AATGTGTTTTACCCAGCACG-3′ and reverse, 5′-TGCTTTGGTCTATTTTAGTTCC-3′; *CYBB* ex13: forward, 5′-TAGACATCTCATCCCAAAGC-3′ and reverse, 5′-TTATTTGAGCATTTGGCAGC-3′; *XK* ex1: forward, 5′-TTTCCCAAGATAGGACCC-3′ and reverse, 5′-GTTGAACCACAAGAAACTGC-3′.

aCGH analysis

aCGH measurements used the Agilent Genomic DNA Labeling Kit (Agilent Technologies). In brief, 1 μg of each of the patient and control DNA (patients 1, 2, and 3: gender non-matched reference controls, patients 4 and 5: gender matched reference controls) were digested with two restriction enzymes (AluI and RsaI; Life Technologies, Carlsbad, CA). Random-primed DNA labeling was performed according to the manufacturer's recommended protocol using Cy3-dUTP for patient DNA and Cy5-dUTP for control DNA. After reacting at 37°C for 2 hrs, labeled patient and control DNA were purified using DNA Microcon YM-3-filter units (Millipore, Billerica, MA), mixed, and human Cot-1 DNA (Life Technologies) and hybridization buffer (Agilent Technologies) were added. The mixed samples were applied to microarray slides (Human Genome CGH Microarray 244A, Agilent Technologies) and the microarray slides were hybridized in Agilent SureHyb chambers at 65°C for 40 hrs. After a second washing operation and microarray scanning (Agilent DNA microarray scanner and Agilent Scan Control Software), images were extracted using the Feature Extraction Software (version 9.5.3.1; Agilent Technologies) and imported into the Agilent CGH-Analytics V3.5.14 Software for analysis, and statistically significant CNVs were determined using the aberration detection module (ADM)-2 algorithm. For details of the statistical algorithm, the Agilent Technologies user's manual is available (http://www.agilent.com/chem/goCGH). Copy-number size was measured as the difference between the first and last probe position in the region deleted using the algorithm. The chromosome resolution of DNA variants with this method averaged 6.4 kb.

Determining of breakpoints

Breakpoints were analyzed in patients 1 and 2. Deletions of telomeric and centromeric breakpoints revealed by the aCGH results of patient 1 were determined by the previously reported step-by-step PCR method [4] using the TAKARA Ex Taq (Takara Bio, Tokyo, Japan). Finally, after amplification by PCR with primers set to sandwich the telomeric and centromeric breakpoints, direct sequence analysis (ABI 310, Life Technologies) of the PCR product was performed. In patient 2, on the other hand, as shown in the results, it was not possible to find the breakpoints by the method described above. To determine the deletion breakpoints, a DNA walking analysis was conducted according to the manufacturer's instructions (DNA Walking Kit; Seegene, Rockville, MD). For patient 2, gene-specific primary 1stF 5′-GGAATCTACTGTGGAAATGC-3′, 2ndF 5′-TGTTACAT-CATGCTGAAACTATG-3′, 3rdF 5′-TCCCGCCAAAATATG-CAAC-3′ and nested primers designed based on the base sequence near the telomeric breakpoint region were used for PCR amplification in combination with primary and nested PCR to Genome Walker Adaptors. To confirm the results, gene-specific primes were designed to straddle the deletion breakpoints, and PCR products were amplified from genomic DNA. PCR products were analyzed by direct sequence analysis. Gene sequences obtained from the analysis were searched for genetic information using the NCBI's BLAST Human Sequences (http://www.ncbi.nlm.nih.gov/genome/seq/BlastGen/BlastGen.). Androgen Receptor in the X-chromosome (the HUMARA region) of patient 5 was analyzed by methylation specific PCR and examined for skewed lyonization [12].

Acknowledgments

We would like to thank all participating patients and staffs of collaborating institutes.

Author Contributions

Conceived and designed the experiments: TA TO HO. Performed the experiments: TA HY. Analyzed the data: TA HY. Contributed reagents/materials/analysis tools: HN JK MU T. Kubota TS T. Kizaki. Wrote the paper: TA HO.

References

1. Johnston RB, Jr. (2001) Clinical aspects of chronic granulomatous disease. Curr Opin Hematol 8: 17–22.
2. Roos D, Kuhns DB, Maddalena A, Roesler J, Lopez J, et al. (2010) Hematologically important mutations: X-linked chronic granulomatous disease (third update). Blood Cells Mol Dis 45: 246–265.
3. Nunoi H (2007) Two breakthroughs in CGD studies. Jap J Clin Immunol 30: 1–10.
4. Yamada M, Arai T, Oishi T, Hatana N, Kobayashi I, et al. (2010) Determination of the deletion breakpoints in two patients with contiguous gene syndrome encompassing CYBB gene. Eur J Med Genet 53: 383–388.
5. del Gaudio D, Yang Y, Boggs BA, Schmitt ES, Lee JA, et al. (2008) Molecular diagnosis of Duchenne/Becker muscular dystrophy: enhanced detection of dystrophin gene rearrangements by oligonucleotide array-comparative genomic hybridization. Hum Mutat 29: 1100–1107.
6. Shchelochkov OA, Li FY, Geraghty MT, Gallagher RC, Van Hove JL, et al. (2009) High-frequency detection of deletions and variable rearrangements at the ornithine transcarbamylase (OTC) locus by oligonucleotide array CGH. Mol Genet Metab 96: 97–105.
7. Simon KC, Noack D, Rae J, Curnutte J, Sarraf S, et al. (2005) Long polymerase chain reaction-based fluorescence in situ hybridization analysis of female carriers of X-Linked chronic granulomatous disease deletions. J Mol Diagn 7: 183–186.
8. Kabuki T, Kawai T, Kin Y, Joh K, Ohashi H, et al. (2003) A case of Williams syndrome with p47-phox-deficient chronic granulomatous disease. Jap J Clin Immunol 26: 299–303.
9. Srour M, Bejjani BA, Rorem EA, Hall N, Shaffer LG, et al. (2008) An instructive case of an 8-year-old boy with intellectual disability. Semin Pediatr Neurol 15: 154–155.
10. Korenberg JR, Rykowski MC (1988) Human genome organization: Alu, LINES, and the molecular structure of metaphase chromosome bands. Cell 53: 391–400.
11. Mazzarella R, Schlessinger D (1998) Pathological consequences of sequence duplications in the human genome. Genome Res 8: 1007–1021.
12. Kubota T, Nonoyama S, Tonoki H, Masuno H, Imaizumi K, et al. (1999) A new assay for the analysis of X-chromosome inactivation based on methylation-specific PCR. Hum Genet 104: 49–55.
13. Takada H, Kanegane H, Nomura A, Yamamoto K, et al. (2004) Female agammaglobulinemia due to the Bruton tyrosine kinase deficiency caused by extremely skewed X-chromosome inactivation. Blood 103: 185–187.
14. Yoshida M, Yorifuji T, Mituyoshi I (1998) Skewed X inactivation in manifesting carriers of Duchenne muscular dystrophy. Clin Genet 52: 102–107.
15. Gono T, Yazaki M, Agematsu K, Matsuda M, Yasui K, et al. (2008) Adult onset X-linked chronic granulomatous disease in a woman patient caused by a de novo mutation in paternal-origin CYBB gene and skewed inactivation of normal maternal X chromosome. Inter Med 47: 1053–1056.
16. Lewis EM, Singla M, Sergeant S, Koty PP, McPhail LC (2008) X-linked chronic granulomatous disease secondary to skewed X chromosome and late presentation. Clin Immunol 129: 372–380.
17. Anderson-Cohen M, Holland SM, Kuhns DB, Fleisher TA, Ding L, et al. (2003) Severe phenotype of chronic granulomatous disease presenting in a female with a de novo mutation in gp91-phox and a non familial, extremely skewed X chromosome inactivation. Clin Immunol 109: 308–317.
18. Francke U, Ochs HD, De Martinville B, Giacalone J, Lindgren V, et al. (1985) Minor Xp21 chromosome deletion in a male associated with expression of duchenne muscular dystrophy, chronic granulomatous disease, retinitis pigmentosa, and McLeod syndrome. Am J Hum Genet 37: 250–267.
19. Saunier S, Calado J, Benessy F, Silbermann F, Heilig R, et al. (2000) Characterization of the NPHP1 Locus: Mutation Mechanism Involved in Deletion in Familial Juvenile Nephronophthisis. Am J Hum Genet 66: 778–789.
20. Shchelochkov OA, Cooper ML, Ou Z, Peacock S, Yatsenko SA, et al. (2008) Mosaicism for r(X) and del(X)del(X)(p11.23)dup(X) (p11.21p11.22) provides insight into the possible mechanism of rearrangement. Mol Cytogenet 1: 16.
21. Bonaglia MC, Giorda R, Massagli A, Galluzzi R, et al. (2009) A familial inverted duplication/deletion of 2p25.1-25.3 provides new clues on the genesis of inverted duplications. Eur J Hum Genet 17: 179–186.
22. Lee JA, Carvalho CM, Lupski JR (2007) A DNA replication mechanism for generating nonrecurrent rearrangements associated with genomic disorders. Cell 131: 1235–1247.
23. Hastings PJ, Lupski JR, Rosenberg SM, Ira G (2009) Mechanisms of change in gene copy number. Nat Rev Genet 10: 551–564.

J Clin Immunol (2012) 32:39–49
DOI 10.1007/s10875-011-9600-0

Successful Treatment with Infliximab for Inflammatory Colitis in a Patient with X-linked Anhidrotic Ectodermal Dysplasia with Immunodeficiency

Tomoyuki Mizukami · Megumi Obara · Ryuta Nishikomori · Tomoki Kawai · Yoshihiro Tahara · Naoki Sameshima · Kousuke Marutsuka · Hiroshi Nakase · Nobuhiro Kimura · Toshio Heike · Hiroyuki Nunoi

Received: 23 July 2011 / Accepted: 15 September 2011 / Published online: 13 October 2011

Abstract X-linked anhidrotic ectodermal dysplasia with immunodeficiency (X-EDA-ID) is caused by hypomorphic mutations in the gene encoding nuclear factor-κB essential modulator protein (NEMO). Patients are susceptibile to diverse pathogens due to insufficient cytokine and frequently show severe chronic colitis. An 11-year-old boy with X-EDA-ID was hospitalized with autoimmune symptoms and severe chronic colitis which had been refractory to immunosuppressive drugs. Since tumor necrosis factor (TNF) α is responsible for the pathogenesis of NEMO colitis according to intestinal NEMO and additional TNFR1 knockout mice studies, and high levels of TNFα-producing mononuclear cells were detected in the patient due to the unexpected gene reversion mosaicism of NEMO, an anti-TNFα monoclonal antibody was administered to ameliorate his abdominal symptoms. Repeated administrations improved his colonoscopic findings as well as his dry skin along with a reduction of TNFα-expressing T cells. These findings suggest TNF blockade therapy is of value for refractory NEMO colitis with gene reversion.

Keywords NEMO colitis · infliximab · gene reversion

Introduction

X-linked anhidrotic ectodermal dysplasia with immunodeficiency (X-EDA-ID) is a rare inherited disease caused by hypomorphic mutations in the gene encoding nuclear factor-κB

Electronic supplementary material The online version of this article (doi:10.1007/s10875-011-9600-0) contains supplementary material, which is available to authorized users.

T. Mizukami · M. Obara · H. Nunoi (✉)
Division of Pediatrics, Department of Reproductive and Developmental Medicine, Faculty of Medicine, University of Miyazaki,
5200 Kihara, Kiyotake,
Miyazaki 889-1692, Japan
e-mail: h-nunoi@fc.miyazaki-u.ac.jp

T. Mizukami
Kumamoto Saishunso National Hospital,
Kumamoto, Japan

R. Nishikomori · T. Kawai · T. Heike
Department of Pediatrics,
Kyoto University Graduate School of Medicine,
Kyoto, Japan

Y. Tahara
Department of Gastroenterology and Hematology,
Faculty of Medicine, University of Miyazaki,
Miyazaki, Japan

N. Sameshima · K. Marutsuka
Department of Pathophysiology, Faculty of Medicine,
University of Miyazaki,
Miyazaki, Japan

H. Nakase
Department of Gastroenterology and Hepatology,
Kyoto University Graduate School of Medicine,
Kyoto, Japan

N. Kimura
Division of Medical Oncology, Hematology and Infectious Disease, Department of Medicine, Fukuoka University,
Fukuoka, Japan

(NF-κB) essential modulator (NEMO), which is the regulatory subunit of IκB kinase [1–3]. Mutations of NEMO can cause an impaired capacity to activate NF-κB, resulting in defects in ectodermal differentiation and innate and adaptive immunity [4, 5]. Affected patients generally show multiple developmental anomalies in ectodermal tissues such as sparse hair, hypodontia with conical teeth, and anhidrosis or hypohidrosis due to lack of sweat glands. These patients also suffer from severe life-threatening infections in various sites caused by Gram-positive or Gram-negative bacteria or mycobacteria. Immunological abnormalities are characterized by defects in the production of proinflammatory cytokines in response to lipopolysaccharide (LPS) stimulation, hypogammaglobulinemia, specific antibody deficiency, and natural killer cell dysfunction. Hematopoietic stem cell transplantation for X-EDA-ID has been employed as a curative treatment [6–10], but has sometimes resulted in engraftment failure.

NEMO colitis, which is inflammatory colitis associated with mutated NEMO protein [11], is found in one fifth of all X-EDA-ID patients [12] and is usually reported as inflammatory bowel disease (IBD), atypical colitis, or Behcet's disease [6, 11, 13]. The onset of inflammatory colitis occurs early in childhood and often causes failure to thrive [2, 5–7, 9, 11–13]. The age of onset of colitis in X-EDA-ID is earlier than that of Crohn's disease, ulcerative colitis, or chronic granulomatous disease [14]. Histological examination reveals active colitis with abundant neutrophilic infiltration, and the colitis usually improves with corticosteroids but not with antimicrobial agents [6, 11]. Susceptibility to colitis remains after hematopoietic stem cell transplantation [6, 9].

Recently, Nenci et al. demonstrated that mice lacking NEMO in intestinal epithelial cells developed spontaneous severe colitis [15]. However, an additional lack of tumor necrosis factor (TNF) receptor-1 in these mice inhibited intestinal inflammation. These interesting findings suggest that TNFα plays a role in the progression of NEMO colitis and that TNF blockade therapy would be a promising treatment.

We describe here an X-EDA-ID boy suffering from severe intractable colitis who improved dramatically following treatment with a chimeric anti-TNFα monoclonal antibody, infliximab. Infliximab administration reduced all symptoms relating to inflammatory colitis, not only frequent diarrhea and severe abdominal pain, but also inflammatory findings by colonoscopy. These effects have lasted for more than 2 years with regular administrations of infliximab.

Methods

Cell Preparation and Culture

Peripheral blood mononuclear cells (PBMCs) were isolated from peripheral blood from our X-EDA-ID patient and his mother using Ficoll-Paque gradient centrifugation. PBMCs were suspended in RPMI 1640 medium (Sigma-Aldrich, USA) and non-adherent cells were used to obtain stimulated T cells. Adherent cells were cultured for 10 days with 500 U/mL granulocyte-macrophage colony-stimulating factor (GM-CSF) (Peprotech, USA) to induce monocyte proliferation. T cells were stimulated for 48 h with 1-μg/mL phytohemaggulutinin (PHA) (Seikagaku Kogyo, Japan) and then for 8 days with 10-U/mL recombinant human interleukin (IL)-2 (Genzyme Techne, USA).

Cytokine Production Assay

PBMCs from our patient and healthy volunteers were incubated with LPS (1 μg/mL) (Sigma-Aldrich) at a concentration of 1×10^6 cells/mL at 37°C for 24 h. The concentration of TNFα in supernatant was measured using human BD OptEIA enzyme-linked immunosorbent assay kits (Becton-Dickinson, USA).

Mutation Analysis and Reversion Analysis

Genomic DNA from our patient and his mother was extracted from PBMCs, stimulated T cells, and stimulated monocytes using Puregene DNA purification kit (Gentra/Qiagen, USA); total RNA was extracted using TRIzol, according to the manufacturer's instructions (Invitrogen, USA). Complementary DNA (cDNA) was synthesized from total RNA with TaKaRa RNA PCR™ Kit (AMV) (Takara, Japan). Polymerase chain reaction (PCR) of genomic DNA and cDNA was performed using TaKaRa LA Taq (TaKaRa) with primers to amplify between exon 2 and exon 4 in the *IKBKG* gene. PCR primers were as follows: c1F, 5′-GCGCTCCTGAGACCCTCCAG-3′; c2R, 5′-GAGGAGAAGGAGTTCCTCAT-3′; G3F, 5′-CCCAGCTCCCCTCCACTGTC-3′; G4R, 5′-AACCCTG GAAGGGGTCTCCGGAG-3′. Genomic DNA was denatured at 94°C for 3 min, followed by 35 cycles of denaturation at 94°C for 30 s, annealing at 64°C for 30 s, and elongation at 68°C for 2 min 30 s, and a final extension for 7 min at 72°C using G3F and G4R primers. cDNA was denatured at 94°C for 1 min, followed by 35 cycles of denaturation at 94°C for 30 s, annealing and elongation at 68°C for 1 min, and a final extension for 5 min at 68°C using c1F and c2R primers. After gel electrophoresis and visualization, targeted bands were extracted and sequenced using ABI Big-Dye Terminator (Applied Biosystems, USA).

To analyze the reversion of mutation, we used our X-EDA-ID patient's PBMCs and stimulated cells. Mononuclear cells sorted with FACSVANTAGE (Becton-Dickinson) were used only at analysis after 12 months of infliximab treatment. PCR products were subcloned using a TOPO

TA cloning kit (Invitrogen) and sequenced as described above.

Reporter Assay for Detecting a Mutant NEMO Function: NEMO-NF-κB Luciferase Reporter Assay

NEMO cDNAs from a healthy volunteer and our patient were subcloned into the p3xFLAG-CMV14 vector (Sigma), respectively. NEMO null rat fibroblast cells (kindly provided by Dr. S. Yamaoka) were plated at a density of 3×10^4 cells/well in a 24-well culture dish and were transfected with 200 ng of plasmid, containing 40 ng of NF-κB reporter plasmid (pNF-κB-Luc; BD Biosciences Clontech, USA), 2 ng of a *NEMO* mutant expression construct, 148 ng internal control for normalization of transfection efficiency (pRL-TK; Toyo Ink, Japan), and the corresponding mock vector, using the FuGENE® HD Transfection Reagent (TOYO-B-Net, Japan) according to the manufacturer's protocol. At 12 h after transfection, the cells were stimulated with 15 ng/mL LPS for 4 h and the NF-κB activity was measured using the PicaGene® Dual SeaPansy assay kit (TOYO-B-NET) according to the manufacturer's protocol. Experiments were performed in triplicate and firefly luciferase activity was normalized to Renilla luciferase activity.

Vβ and Vα Analysis of T Cells

T cell receptor (TCR) β and α chain variable region (Vβ and Vα) repertoires were analyzed by a reverse transcription polymerase chain reaction (RT-PCR) method as described [16]. Briefly, each Vβ fragment (from Vβ1 to Vβ20) or Vα fragment (from Vα1 to Vα18, Vα21, and Vα24) was prepared from a series of HBVT/HBVP or HAVT/HAVP plasmids originating from thymus or peripheral T cells [17] and was dotted on filters. PCR products obtained from the patient by RT-PCR were labeled by α-^{32}P-dCTP and hybridized to the filters. Using densitometry, a semiquantitative assessment of V gene usage was made from the amounts of hybridized products.

Flow Cytometry

Peripheral blood samples were analyzed by three-color flow cytometry. Cells were stained with monoclonal antibodies to the following cell surface markers: CD3, CD4, CD8, CD19 (Becton-Dickinson), and CD14 (eBioscience, USA). Flow cytometry analysis of intracellular NEMO protein was performed as described previously [18]. Flow cytometric data from the stained cells were collected by FACScalibur and analyzed with CellQuest software (Becton-Dickinson).

Intracellular Cytokine Staining

Whole blood samples from our X-EDA-ID patient and healthy donors were stimulated with 1-μg/mL ionomycin (Sigma-Aldrich) and 25-ng/mL phorbol 12-myristate 13-acetate (PMA) (Sigma-Aldrich) in the presence of 10-μg/mL brefeldin A (Sigma-Aldrich) for 4 h. Cultured cells were stained with monoclonal antibodies against CD4 and CD8 for 30 min at room temperature. Stained cells were fixed and permeabilized with BD Lysing solution (Becton-Dickinson) and incubated with anti-TNFα monoclonal antibody or IgG1 isotypic control (Becton-Dickinson). Cells were analyzed by flow cytometry as described above. Analysis of intracellular TNFα in CD14+ cells was performed after stimulation with LPS (1 μg/mL) at 37°C for 4 h.

Endoscopy and Immunohistochemical Staining

Endoscopy was performed with the consent of legal guardians. Colon biopsies were obtained at regions of visual abnormalities. Formalin-fixed paraffin-embedded tissues blocks were cut into 2-μm sections and stained with hematoxylin and eosin. Subsequently, immunohistochemical analysis using the following primary antibodies with optimized experimental protocols was performed: CD3ε (DAKO, Denmark, rabbit, polyclonal, diluted 1:100, incubated for 24 h at 4°C after microwave heat-induced antigen retrieval for 40 min in pH 6.0 citrate buffer), CD79a (DAKO, mouse, monoclonal, 1:100, microwave for 40 min, pH 6.0), CD68 (DAKO, mouse, monoclonal, 1:50, proteinase K (DAKO) for 10 min at room temperature), CD4 (Novocastra, USA, 1:100, microwave for 40 min, pH 9.0 (NICHIREI BIOSCIENCES, Japan)), CD8 (DAKO, mouse, monoclonal, 1:100, microwave for 40 min, pH 9.0), and TNFα (Santa Cruz Biotechnology, USA, goat, polyclonal, 1:200, microwave for 40 min, pH 6.0). An Envision-HRP Detection kit (DAKO) was used for visualization, except for anti-TNFα, which was visualized using donkey biotin conjugated anti-goat secondary antibody (Jackson ImmunoResearch Laboratories, USA) and LASB2-System/HRP kit (DAKO).

Infliximab Treatment

Infliximab treatment for our X-EDA-ID patient was approved by the medical ethics committee of the University of Miyazaki. We obtained written consent concerning treatment from both the patient and his guardian. Before initiating infliximab, we confirmed that he had no severe infection including tuberculosis according to laboratory data, mycobacterium culture test, skin tuberculin test, and chest computed tomography. Cardiac dysfunction was excluded by echocardiography and electrocardiogram.

Infliximab was given intravenously over 2 h at a dose of 5 mg/kg on 0, 2, and 6 weeks, with follow-up treatments every 7–8 weeks depending on clinical symptoms. The patient was monitored regularly throughout the infliximab treatment.

Results

Case

The patient was born to unrelated Japanese parents after an uncomplicated pregnancy of 41 weeks. There was no history of any first-degree relative diagnosed with incontinentia pigmenti. On the first day after birth, he presented high fever with a markedly increased white blood cell count ($40\times10^3/\mu L$) and was treated successfully with antibiotics. He has had a history of recurrent, severe infections including varicella at 3 months of age, penicillin-resistant *Streptococcus pneumoniae* meningitis at 6 months of age, and zoster at 8 months of age. Persistent diarrhea was also observed.

He was introduced to our hospital at 8 months of age for examination of his immunological status. On admission, he showed a marked increase in both white blood cells ($31.9\times10^3/\mu L$) and platelets ($872\times10^3/\mu L$). Peripheral blood T cell count was decreased (CD3-positive cells, 25.8%), and B cell count was highly increased (CD20-positive cells,: 69.2%). PHA induced a normal proliferation response of T cells, and concentrations of immunoglobulins were within the normal range except IgD (less than 0.2 mg/dL). Natural killer cell activity was markedly impaired. Superoxide-generating ability from neutrophils was intact. LPS-induced TNFα production from patient's PBMC was impaired (Fig. 1a). Interferon (IFN) γ-producing lymphocytes were also reduced apparently at 8 months of age (Table I). All the genes involving in the IL-12 signal pathway, including *IL12RB1*, *IL12RB2*, *JAK2*, and *STAT4* were sequenced, but no mutations were found (data not shown). Surprisingly, both IFNγ-producing T cells and natural killer cells had expanded significantly by 11 months of age (Table I). In addition, we observed that he had ectodermal dysplasia including anhidrosis and conical teeth (Supplementary Fig. 1). A skin biopsy revealed the absence of eccrine sweat glands. When he was 3 years old, a G505C (A169P) missense mutation in his *IKBKG* gene was confirmed and diagnosed as X-EDA-ID. His mother was a carrier. An expression of mutant NEMO protein was not markedly

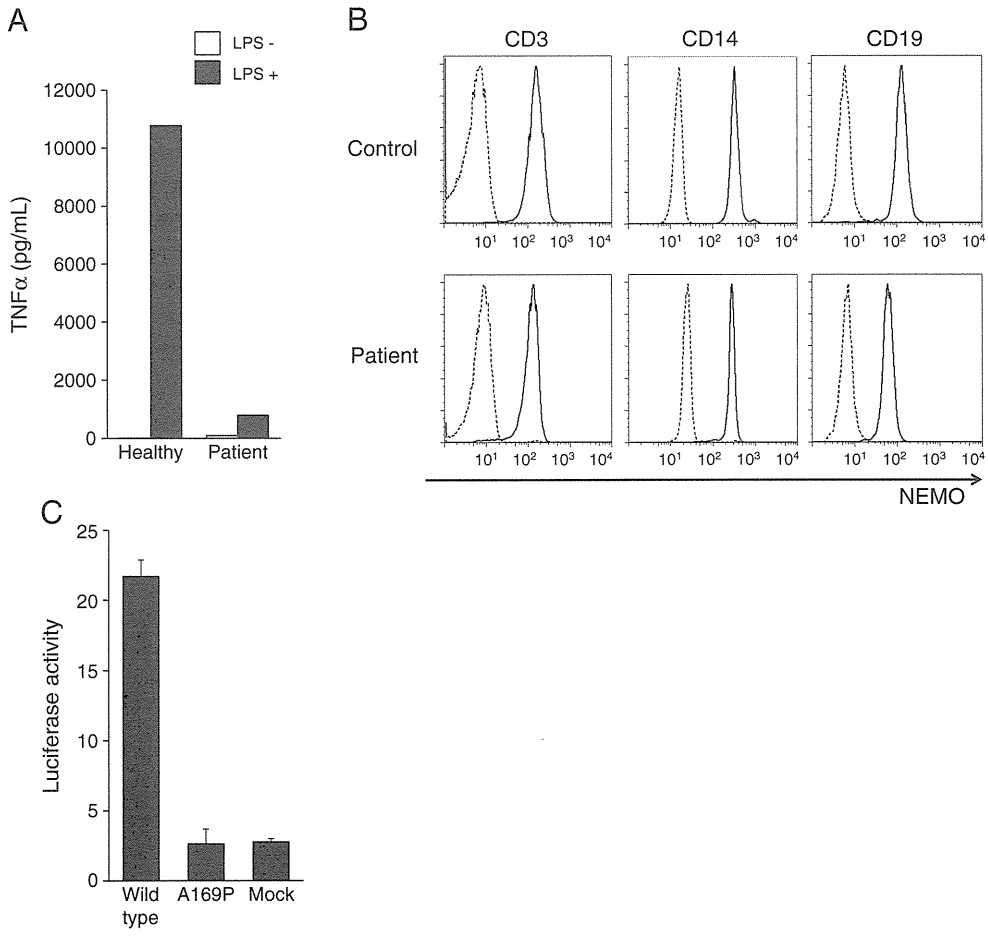

Fig. 1 Analysis of mutant NEMO protein. **a** Reduced production of TNFα from LPS-stimulated PBMCs. PBMCs from our patient and healthy volunteer were stimulated with LPS (1 μg/mL). **b** Analysis of NEMO protein expression using flow cytometry. Intracellular NEMO protein in PBMCs from the patient was not reduced markedly. **c** The result of NEMO-NF-κB luciferase reporter assay. The activity of mutant NEMO in the patient was almost defective. Mock vectors and wild-type NEMO were used as controls. *Error bars* indicate SD

Table I Proportion of IFNγ-expressing T and NK cells in the patient

Age	$IFN\gamma^+/IL\text{-}4^-$		
	CD4 (%)	CD8 (%)	CD56 (%)
8 months	1.14	8.83	2.00
11 months	3.18	70.40	66.29
3 years 11 months	11.89	65.48	82.79
Healthy control	15	60–80	80–90

reduced by flow cytometer (Fig. 1b), but the activity of mutant NEMO was almost defective which was confirmed by a mutant NEMO-NF-κB luciferase reporter assay (Fig. 1c). He has been prescribed prophylactic cotrimoxazole before and after the diagnosis.

He presented with chest pain, erythema, polyarthritis, continuous high fever refractory to antibiotics, and marked elevation of C-reactive protein (7.4 mg/dL) at 4 years of age. Autoantibodies such as anti-centromere antibody were detected transiently. Chest computed tomography revealed multiple nodular shadows resembling bronchiolitis obliterans organizing pneumonia. The repertoire of T cell receptor showed high expression of limited Vβ subsets (Supplementary Fig. 2). Combination therapy using corticosteroids, cyclosporine A, and methotrexate was effective and was continued to control his symptoms.

Severe abdominal pain and intractable frequent diarrhea recurred when the corticosteroid dose was reduced, and he presented perianal fistula at 8 years of age. A mild elevation was observed in both erythrocyte sedimentation rate and C-reactive protein under the preceding immunosuppressive treatments (Table II). No significant pathogen was detected by stool culture and the use of antibiotics and antifungal drugs resulted in no improvement in clinical symptoms.

Endoscopic and Microscopic Findings of the Colon

Colonic endoscopy revealed many polyp-like lesions with mucosal redness and edema at the sigmoid/descending junction (Fig. 2). A longitudinal ulcerative lesion found in the sigmoid colon was suggestive of Crohn's disease. Passing the endoscope beyond these obstructive clusters of polyps was difficult; therefore, we could not observe the upper part of the colon. Neither stenosis nor ulcer formation was observed by intestinal radiocontrast analysis.

Histopathological examination of the colonic biopsied specimens showed diffuse lymphoplasmacytic infiltration, superficial edema, and hyperemia in lamina propria. Foamy cells and some eosinophils were also seen (Fig. 3a, b). No definite neutrophilic infiltration, crypt abscesses, or granulomatous lesions were observed. Cultures from biopsied specimens yielded neither bacterial nor fungal growth.

Immunohistochemical staining revealed predominant infiltration of CD79a-positive, plasma cells in the lamina propria. Infiltration of CD68-positive macrophages and CD3-positive T cells was also observed (Fig. 3c–g).

Detection of TNFα-Producing Cells in the Lamina Propria and Peripheral Blood

To investigate the possibility that TNFα blockade therapy can ameliorate inflammatory colitis as well as NEMO-deficient mice as suggested by previous analysis [15], we analyzed TNFα-producing mononuclear cells in the lamina propria in the colon of our patient. Immunohistochemical staining showed abundant TNFα in infiltrated mononuclear cells in the lamina propria (Fig. 3h) which would be associated with progression of inflammatory colitis.

We also analyzed TNFα-producing T cells and monocytes in the peripheral blood (Fig. 4a). The majority (72.49%) of CD4-positive T cells in our patient expressed intracellular TNFα, while 40% to 70% of CD4-positive T cells expressed TNFα in adults with IBD in our study. Forty-eight percent of CD8-positive T cells in our patient expressed TNFα. CD14-positive monocytes from our patient expressed small amounts of intracellular TNFα after LPS stimulation, while similarly treated CD14-positive cells from healthy subjects expressed abundant TNFα (Fig. 4b).

Reversion Analysis

Nishikomori et al. reported that in an X-EDA-ID patient, the mutation had been reverted to the normal state in IFNγ-

Table II Laboratory data on admission (8 years old)

WBC	13,600/μL	CD3	76.2%	IgG	790 mg/dL
Neutrophils	10,200/μL	CD4	22.2%	IgA	666 mg/dL
Lymphocytes	1,632/μL	CD8	58.3%	IgM	71 mg/dL
Monocytes	952/μL	CD19	4.8%	IgD	<0.6 mg/dL
Hemoglobin	12.0 g/dL	CD20	3.8%	C3	134 mg/dL
Platelets	84.7×10^4/μL	CD16	0.5%	C4	46 mg/dL
		CD56	33.6%	CH50	56 U/mL
		HLA-DR	26.5%	ESR	43 mm/h

WBC white blood cell, *CH50* total complement activity, *ESR* erythrocyte sedimentation rate

Fig. 2 Findings of colonoscopy performed before initial treatment with infliximab. Colonoscopy revealed polyp-like lesions with mucosal redness and edema at the sigmoid/descending junction (*left panel*). A longitudinal ulcer (*arrowhead*) was found in the sigmoid colon (*center panel*). Same segment as in the *center panel* after indigo carmine dye (*right panel*)

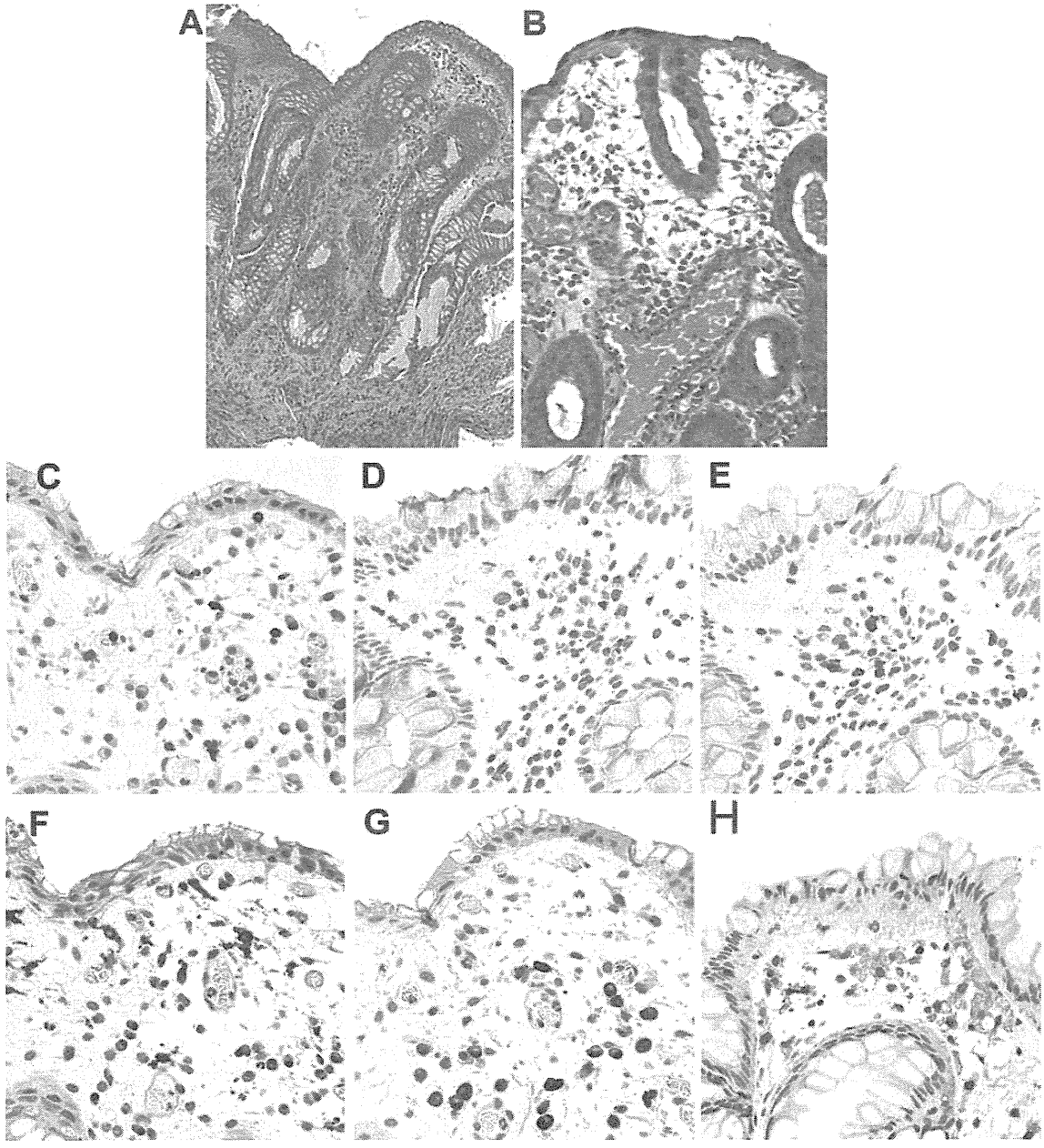

Fig. 3 Microscopic findings of affected colonic specimens. **a**, **b** Hematoxylin and eosin staining. **a** and **b** are low-power field and high-power field views, respectively. **c**–**h** Staining profiles of cellular surface antigens: **c** CD3ε, **d** CD4, **e** CD8, **f** CD68, and **g** CD79a. **h** Staining with anti-human TNFα antibody

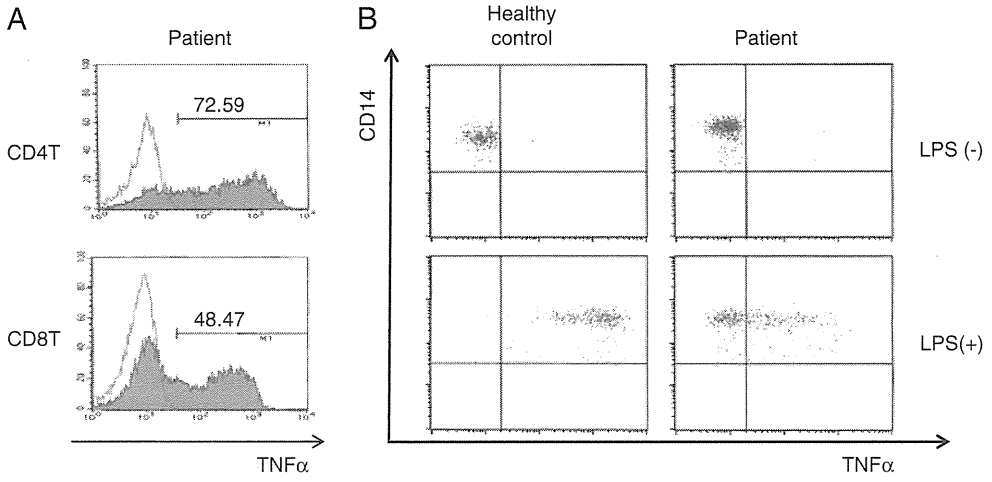

Fig. 4 Analysis of TNFα-producing mononuclear cells in peripheral blood. **a** TNFα-expressing T cells increased markedly before infliximab treatment. PBMCs were stimulated with ionomycin and PMA for 4 h in the presence of brefeldin A then stained for intracellular TNFα. For FACS analysis, gates were set on lymphocytes according to forward and side scatter properties. Representative histograms of TNFα expression in stimulated (*solid histograms*) or unstimulated (*black line histograms*) T cells. The proportion of TNFα-positive CD4-positive T cells in adult IBD patients is 40–70%. **b** The percentage of TNFα-positive monocytes was examined. Cells from our patient and healthy volunteer were incubated with or without LPS for 4 h in the presence of brefeldin A. Monocytes were identified by CD14. Approximately 50% of stimulated monocytes produced a small amount of TNFα

expressing T cells [18]. Our patient showed expansion of IFNγ-expressing T cells during infancy and an increase in TNFα-producing T cells at that time. We hypothesized that the A169P mutation in the *IKBKG* gene had been reverted to wild type and that the reverted T cells had expanded in our patient. Indeed, before initiating infliximab treatments, reversion mutation was detected in 23/67 (34%) from non-stimulated PBMCs (Table III). At 24 months after the initiation, reversion mutation was detected in both messenger RNA (mRNA) and genomic DNA from lymphocytes stimulated with PHA and IL-2 for 10 days, whereas only mutated mRNA was identified from non-stimulated lymphocytes (Fig. 5). Reverted mRNA was observed in CD3-positive T cells. Sex chromosome analysis with fluorescent in situ hybridization revealed no maternal cells and therefore graft-versus-host disease secondary to maternal–fetal transfusion was unlikely. These findings suggest that reverted T cells activated NF-κB in response to growth signals and had a growth advantage over mutant cells.

Table III Frequency of reverted clones before and after initiation of infliximab treatments

	Before	After 12 months	After 24 months
PBMCs	23/67 (34%)	nd	2/6 (33%)[a]
CD3	nd	3/16 (19%)	nd
CD14	nd	0/19 (0%)	nd
CD19	nd	0/47 (0%)	nd

nd not done

[a] A result using stimulated mononuclear cells

Reverted T cells decreased with repeated administrations of anti-TNFα monoclonal antibody. In contrast, CD14-positive monocytes and GM-CSF-induced monocyte-derived dendritic cells had no reversion (Table III).

Anti-TNFα Treatment Improved NEMO Colitis

We initially treated NEMO colitis with high dose corticosteroid therapy (2 mg/kg prednisolone, daily) (Fig. 6). However, steroid therapy did not improve clinical symptoms and resulted in compression fracture in the thoracic spine from corticosteroid-induced osteoporosis.

The increase in TNFα-producing T cells suggested the possibility that TNFα blockade therapy would be an effective treatment for the intractable NEMO colitis. After confirming the absence of severe bacterial or mycobacterial infection, we initiated administration of the chimeric anti-TNFα monoclonal antibody, infliximab, to our patient.

Soon after the first infusion of infliximab, abdominal pain disappeared and his appetite recovered. Frequency of diarrhea decreased as administrations of infliximab were repeated (Fig. 6). Colonoscopy after his third administration showed mild improvement of both mucosal redness and edema (Fig. 7a). These mucosal inflammatory findings had almost disappeared after 1-year treatment with infliximab, although polyp-like lesions remained (Fig. 7b).

The proportion of TNFα-producing cells in CD4-positive and CD8-positive T cells markedly decreased by his third infliximab infusion (from 72.6% to 26.7% in CD4-positive T cells and from 48.5% to 23.1% in CD8-positive T cells), and reduction of TNFα-producing cells was

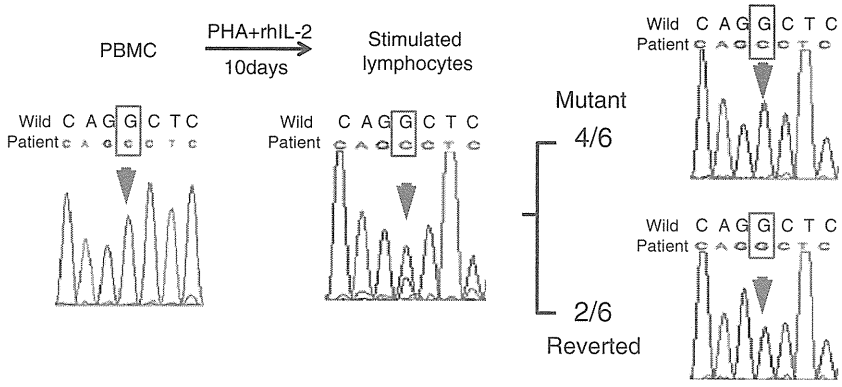

Fig. 5 Reversion analysis of cDNA of gene encoding NEMO isolated from mononuloclear cells after 24 months of infliximab treatment. PBMC was obtained from our patient and incubated with PHA and IL-2 for 10 days. Direct sequence for mRNA encoding NEMO was performed using PBMC and the stimulated mononuclear cells. Before stimulation, no reverted mononuclear cells were detected. After PHA and IL-2 stimulation, reverted mononuclear cells apparently increased. Subcloning of cDNA from stimulated cells showed that two of six cells had reversion of mutation in the gene

associated with improvement of clinical symptoms (Fig. 6). Administration of cyclosporine A was discontinued by the eighth infliximab treatment, and corticosteroid was reduced and then discontinued by the tenth infliximab infusion.

Our patient had one serious adverse event, pneumonia, after his fourth administration of infliximab. *Campylobacter jejuni* was isolated from his blood culture at that time. He was successfully treated with antibiotics and infliximab administration was resumed after confirming resolution of pneumonia. He has been treated safely for more than 2 years with regular administrations of infliximab (once every 7–8 weeks). Neither mycobacterial infections nor severe infusion reactions have been observed.

Discussion

Our patient showed immunodeficiency with very low IFNγ-production during his younger years as shown in Table I and suffered from many opportunistic infections (Zoster virus infection, penicillin-resistant *Streptococcus pneumoniae* meningitis, and other undetermined infections). A novel missense mutation, A169P, in the first coiled-coil domain resulted in defective NEMO function (Fig. 1) and was responsible for recurrent severe infections. However, he later suffered from autoimmune diseases at 4 years of age (bronchiolitis obliterans organizing pneumonia, severe arthritis, and vasculitis) and severe chronic inflammatory colitis at 8 years. Based on the facts that, in the mice model, TNFα played a major role in the pathogenesis of NEMO colitis [15], and that, in our patient, TNFα-producing mononuclear cells in the peripheral blood were markedly increased (Fig. 4a), infliximab was employed for the patient's treatment. This treatment led to improvement in his symptoms and colonoscopic findings for 2 years.

Increases in TNFα-producing cells similar to that seen in other IBD [19] were detected (Fig. 4). We confirmed G/C

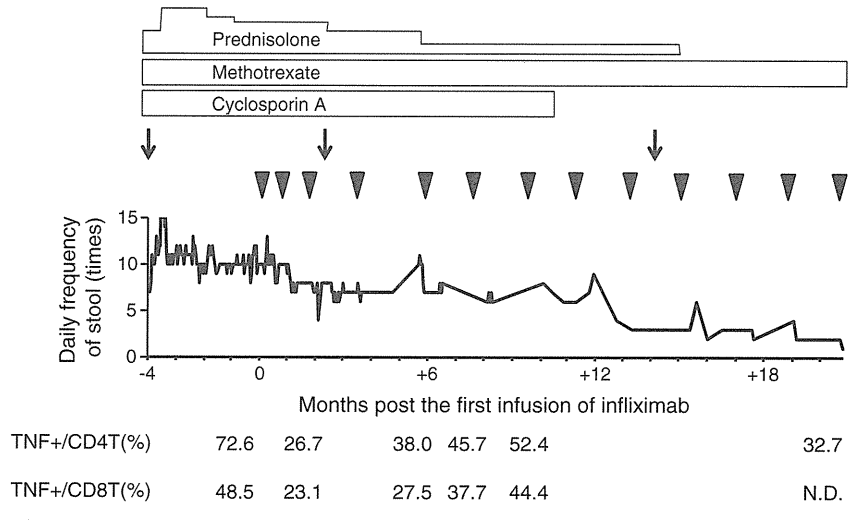

Fig. 6 Clinical course of NEMO colitis after infliximab treatment in our patient. Colonoscopy (*arrows*), administrations of infliximab (*arrowheads*), and other immunosuppressive drugs (*bars*) are indicated. Daily frequency of stools (times) is graphed at the *center*. Changes in the proportion of TNFα-producing T cells in CD4-positive and CD8-positive cells are also indicated at the *bottom*

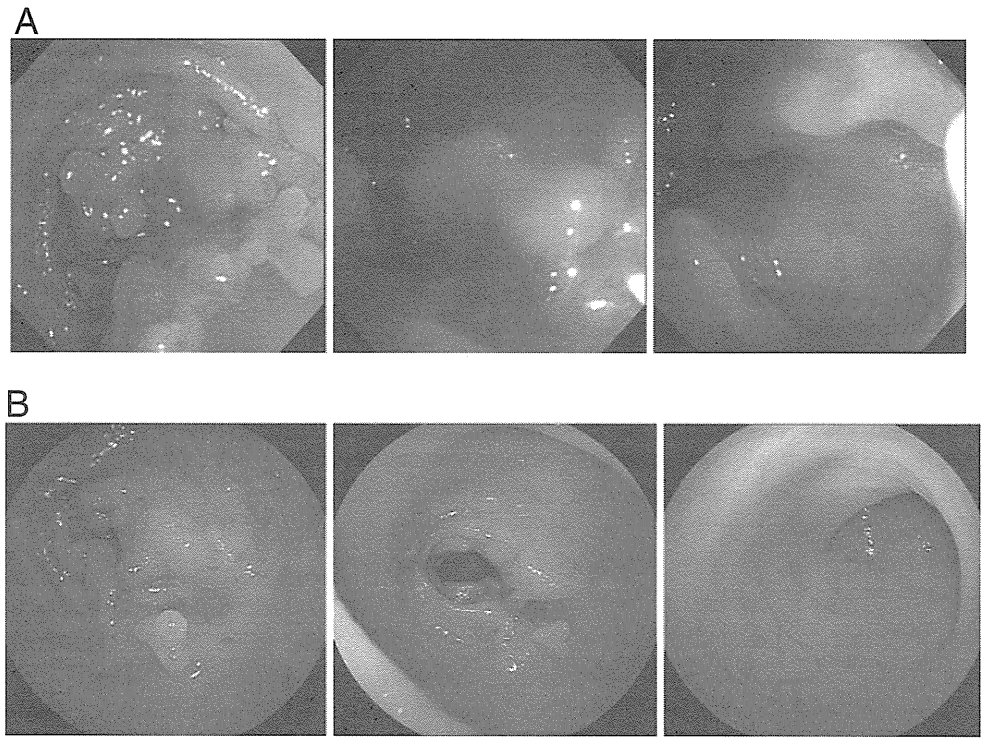

Fig. 7 Findings of colonoscopy after infliximab treatment. **a** Colonoscopy performed after the third infliximab treatment. Mild improvement was observed. Both mucosal redness and edema decreased. However, polyp-like lesions remained. At this point, the patient showed neither abdominal pain nor watery diarrhea. **b** Colonoscopy after 1-year treatment. Almost no mucosal redness or edema. A clear vascular pattern was also observed. Inflammatory polyps could still be found

reversion in T cells after co-stimulation with PHA and IL-2 before and even after infliximab therapy (Table III and Fig. 5). Reversion mosaicism has been reported in primary immunodeficiencies such as X-linked severe combined immunodeficiency [20, 21], adenosine deaminase deficiency [22], *RAG1* deficiency [23], and Wiskott–Aldrich syndrome [24]. Most of these patients reduced the frequency of severe infections and showed survival for longer periods. Our patient also had very few episodes of severe infection after expansion of IFNγ-producing peripheral blood mononuclear cells, contrary to increased susceptibility to diverse pathogens in X-EDA-ID [5, 25]. However, none of the patients with reversion mosaicism involving reverted T cells developed IBD other than X-EDA-ID. Our patient and patients with Omenn's syndrome [21, 23] developed systemic inflammatory conditions and exhibited a restricted TCR repertoire. In our patient, oligoclonal expansion of reverted T cells caused impairment of immune regulation.

According to the report by Nenci et al. in a murine model of intestinal epithelium-specific NEMO deficiency, intestinal epithelial cells exhibit increased sensitivity to TNFα-induced apoptosis and cause disruption of the epithelial barrier if mucosal immune cells have normal immune functions and produce proinflammatory cytokines [15]. They also showed that an additional TNF receptor-1 knockout ameliorated this intestinal inflammation [15]. The pathogenesis of severe colitis in the mouse model seems to be similar to that of our patient. Specifically, NEMO-deficient intestinal epithelium was damaged by TNFα produced from both T cells and macrophages in the lamina propria (shown in Fig. 3c–e, h), and anti-TNFα antibody suppressed progression of intestinal inflammation. Although reversion in peripheral blood monocytes was not confirmed after culture with GM-CSF and analysis of TNFα expression after LPS stimulation, submucosal and peripheral macrophages produced a fair amount of TNFα detectable by immunohistochemistry and flow cytometry (Figs. 3 and 4). Production of TNFα from lamina propria macrophages may be augmented by IFNγ released from reverted T cells.

In addition to the amelioration of clinical symptoms and colonic mucosal inflammation, in our patient, TNF blockade therapy restored his dry skin with thick epidermis to moderately moist skin of normal thickness. Nenci et al. described in another paper using the epidermis-specific NEMO-deficient mice that mice showed severe skin inflammation with thick epidermis and predominant infiltration of inflammatory cells and showed further that an additional knockout of TNFR1 suppressed the inflammatory condition [26]. We postulate that TNFα is also a key cytokine in the pathogenesis of inflammation in diverse epithelial tissues and that infliximab treatment suppresses the TNFα-mediated inflammatory response by inducing apoptosis of TNFα-producing cells [27]. In fact, the patient's peripheral blood TNFα-producing cells reduced along with the improvement of clinical symptoms, and this reduction provided an available marker to assess inflammatory status. Reverted cells in peripheral blood also decreased after repeated anti-TNFα antibody administrations. Unfortunately, we could not obtain consent for re-biopsy so we could not

confirm a vulnerability for apoptosis of intestinal epithelium and lamina propria after the treatment.

Since patients with X-EDA-ID were well known to have increased susceptibility to mycobacterium, and in addition, anti-TNFα monoclonal antibody indeed caused infection-related deaths in a few patients with inflammatory colitis associated with primary immunodeficiencies [28–30], the side effects of anti-TNFα monoclonal antibody treatment should be paid attention to, especially, mycobacterial infections. Before infliximab treatment, we confirmed the absence of active mycobacterial infections by culture tests for mycobacterium including atypical mycobacteria, laboratory examinations, and chest radiographs. He also has no history of Bacillus Calmette-Guérin immunization. Although the patient experienced bacterial pneumonia after his third infliximab infusion, he has not suffered from severe infections for several years. This may be because of the patient's mosaicism of mutated and reverted cells. The risks concerning severe infections and oncogenic effects [31–33] should be considered before employing infliximab for NEMO colitis.

Conclusion

Reversion of mutation in T cells contributes to the pathogenesis of mucosal immunity in NEMO-deficient patients. Moreover, treatment with anti-TNFα monoclonal antibody therapy can improve the symptoms of the disease by both preventing exposure of the mucosa to TNFα and reducing the number of T cells carrying the reverted gene. Anti-TNFα monoclonal antibody therapy provides a promising treatment for intractable NEMO colitis.

Acknowledgments We profoundly thank for Dr. Kazuko Uno of the Louis-Pasteur Medical Research Center in Japan for support of our experiments and Dr. Maiko Kai and Dr. Naoki Karasawa1 for their warm care of patients. This study was supported by a Grant-in-Aid for Scientific Research from the Ministry of Education, Culture, Sports, Science and Technology, Japan.

Conflict of Interests The authors declare no competing financial interests.

References

1. Zonana J, Elder M, Schneider L, et al. A novel X-linked disorder of immune deficiency and hypohidrotic ectodermal dysplasia is allelic to incontinentia pigmenti and due to mutations in IKK-gamma (NEMO). Am J Hum Genet. 2000;67:1555–62.
2. Döffinger R, Smahi A, Bessia C, et al. X-linked anhidrotic ectodermal dysplasia with immunodeficiency is caused by impaired NF-kappaB signaling. Nat Genet. 2001;27:277–85.
3. Jain A, Ma CA, Liu S, et al. Specific missense mutations in NEMO result in hyper-IgM syndrome with hypohydrotic ectodermal dysplasia. Nat Immunol. 2001;2:223–8.
4. Orange JS, Brodeur SR, Jain A, et al. Deficient natural killer cell cytotoxicity in patients with IKK-gamma/NEMO mutations. J Clin Invest. 2002;109:1501–9.
5. Orange JS, Jain A, Ballas ZK, et al. The presentation and natural history of immunodeficiency caused by nuclear factor kappaB essential modulator mutation. J Allergy Clin Immunol. 2004;113:725–33.
6. Pai S, Levy O, Jabara H, et al. Allogeneic transplantation successfully corrects immune defects, but not susceptibility to colitis, in a patient with nuclear factor-kappaB essential modulator deficiency. J Allergy Clin Immunol. 2008;122:1113–1118.e1111.
7. Tono C, Takahashi Y, Terui K, et al. Correction of immunodeficiency associated with NEMO mutation by umbilical cord blood transplantation using a reduced-intensity conditioning regimen. Bone Marrow Transplant. 2007;39:801–4.
8. Mancini AJ, Lawley LP, Uzel G. X-linked ectodermal dysplasia with immunodeficiency caused by NEMO mutation: early recognition and diagnosis. Arch Dermatol. 2008;144:342–6.
9. Fish J, Duerst R, Gelfand E, et al. Challenges in the use of allogeneic hematopoietic SCT for ectodermal dysplasia with immune deficiency. Bone Marrow Transplant. 2009;43:217–21.
10. Permaul P, Narla A, Hornick J, et al. Allogeneic hematopoietic stem cell transplantation for X-linked ectodermal dysplasia and immunodeficiency: case report and review of outcomes. Immunol Res. 2009;44:89–98.
11. Cheng L, Kanwar B, Tcheurekdjian H, et al. Persistent systemic inflammation and atypical enterocolitis in patients with NEMO syndrome. Clin Immunol. 2009;132:124–31.
12. Hanson E, Monaco-Shawver L, Solt L, et al. Hypomorphic nuclear factor-kappaB essential modulator mutation database and reconstitution system identifies phenotypic and immunologic diversity. J Allergy Clin Immunol. 2008;122:1169–1177.e1116.
13. Takada H, Nomura A, Ishimura M, et al. NEMO mutation as a cause of familial occurrence of Behçet's disease in female patients. Clin Genet. 2010;78:575–9.
14. Marks DJ, Miyagi K, Rahman FZ, et al. Inflammatory bowel disease in CGD reproduces the clinicopathological features of Crohn's disease. Am J Gastroenterol. 2009;104:117–24.
15. Nenci A, Becker C, Wullaert A, et al. Epithelial NEMO links innate immunity to chronic intestinal inflammation. Nature. 2007;446:557–61.
16. Nagano M, Kimura N, Ishii E, et al. Clonal expansion of alphabeta-T lymphocytes with inverted Jbeta1 bias in familial hemophagocytic lymphohistiocytosis. Blood. 1999;94:2374–82.
17. Kimura N, Toyonaga B, Yoshikai Y, et al. Sequences and repertoire of the human T cell receptor alpha and beta chain variable region genes in thymocytes. Eur J Immunol. 1987;17:375–83.
18. Nishikomori R, Akutagawa H, Maruyama K, et al. X-linked ectodermal dysplasia and immunodeficiency caused by reversion mosaicism of NEMO reveals a critical role for NEMO in human T-cell development and/or survival. Blood. 2004;103:4565–72.
19. Ogura Y, Imamura Y, Murakami Y, et al. Intracellular cytokine patterns of peripheral blood T cells as a useful indicator of activeness of Crohn's disease. Hiroshima J Med Sci. 2005;54:1–8.
20. Stephan V, Wahn V, Le Deist F, et al. Atypical X-linked severe combined immunodeficiency due to possible spontaneous reversion of the genetic defect in T cells. N Engl J Med. 1996;335:1563–7.
21. Wada T, Yasui M, Toma T, et al. Detection of T lymphocytes with a second-site mutation in skin lesions of atypical X-linked severe combined immunodeficiency mimicking Omenn syndrome. Blood. 2008;112:1872–5.
22. Hirschhorn R, Yang D, Puck J, et al. Spontaneous in vivo reversion to normal of an inherited mutation in a patient with adenosine deaminase deficiency. Nat Genet. 1996;13:290–5.
23. Wada T, Toma T, Okamoto H, et al. Oligoclonal expansion of T lymphocytes with multiple second-site mutations leads to

Omenn syndrome in a patient with RAG1-deficient severe combined immunodeficiency. Blood. 2005;106:2099–101.
24. Ariga T, Kondoh T, Yamaguchi K, et al. Spontaneous in vivo reversion of an inherited mutation in the Wiskott–Aldrich syndrome. J Immunol. 2001;166:5245–9.
25. Filipe-Santos O, Bustamante J, Haverkamp MH, et al. X-linked susceptibility to mycobacteria is caused by mutations in NEMO impairing CD40-dependent IL-12 production. J Exp Med. 2006;203:1745–59.
26. Nenci A, Huth M, Funteh A, et al. Skin lesion development in a mouse model of incontinentia pigmenti is triggered by NEMO deficiency in epidermal keratinocytes and requires TNF signaling. Hum Mol Genet. 2006;15:531–42.
27. Van den Brande J, Braat H, van den Brink G, et al. Infliximab but not etanercept induces apoptosis in lamina propria T-lymphocytes from patients with Crohn's disease. Gastroenterology. 2003;124:1774–85.
28. Nos P, Bastida G, Beltran B, et al. Crohn's disease in common variable immunodeficiency: treatment with antitumor necrosis factor alpha. Am J Gastroenterol. 2006;101:2165–6.
29. Chua I, Standish R, Lear S, et al. Anti-tumour necrosis factor-alpha therapy for severe enteropathy in patients with common variable immunodeficiency (CVID). Clin Exp Immunol. 2007;150:306–11.
30. Uzel G, Orange JS, Poliak N, et al. Complications of tumor necrosis factor-α blockade in chronic granulomatous disease-related colitis. Clin Infect Dis. 2010;51:1429–34.
31. Mackey AC, Green L, Liang LC, et al. Hepatosplenic T cell lymphoma associated with infliximab use in young patients treated for inflammatory bowel disease. J Pediatr Gastroenterol Nutr. 2007;44:265–7.
32. Mackey AC, Green L, Leptak C, et al. Hepatosplenic T cell lymphoma associated with infliximab use in young patients treated for inflammatory bowel disease: update. J Pediatr Gastroenterol Nutr. 2009;48:386–8.
33. Diak P, Siegel J, La Grenade L, et al. Tumor necrosis factor alpha blockers and malignancy in children: forty-eight cases reported to the Food and Drug Administration. Arthritis Rheum. 2010;62:2517–24.

Molecular Immunology 49 (2011) 48–55

Contents lists available at ScienceDirect

Molecular Immunology

journal homepage: www.elsevier.com/locate/molimm

Factor H gene variants in Japanese: Its relation to atypical hemolytic uremic syndrome

Saki Mukai[a], Yoshihiko Hidaka[b], Masako Hirota-Kawadobora[a], Kazuyuki Matsuda[a], Noriko Fujihara[a], Yuka Takezawa[a], Seiko Kubota[a], Kenichi Koike[b], Takayuki Honda[a,c], Kazuyoshi Yamauchi[d,*]

[a] Department of Laboratory Medicine, Shinshu University Hospital, Japan
[b] Department of Pediatrics, Shinshu University School of Medicine, Japan
[c] Department of Laboratory Medicine, Shinshu University School of Medicine, Japan
[d] Department of Medicine, Molecular Clinical Pathology, Graduate School of Comprehensive Human Sciences, University of Tsukuba, Japan

ARTICLE INFO

Article history:
Received 4 April 2011
Received in revised form 19 July 2011
Accepted 20 July 2011
Available online 24 August 2011

Keywords:
Atypical hemolytic syndrome
Factor H
Genetic analysis
Alternative complement pathway
Hemolytic assay

ABSTRACT

Mutations and polymorphisms of factor H gene (*FH1*) are known to be closely involved in the development of atypical hemolytic uremic syndrome (aHUS). Several groups have identified disease risk mutations and polymorphisms of *FH1* for the development of aHUS, and have investigated frequencies of aHUS in a number of ethnic groups. However, such studies on Japanese populations are limited. In the present study, we analyzed *FH1* in Japanese aHUS patients and healthy volunteers, and examined whether those variants impacted on a tendency for the development of aHUS in Japanese populations. Similar to previous studies, we found that a high frequency of *FH1* mutations, located in exon 23 of *FH1*, encodes short consensus repeat 20 in C-terminal end of factor H molecule in patients with aHUS (40%), but not in healthy volunteers. Interestingly, no significant differences in frequency of well-known disease risk polymorphisms for aHUS were observed between healthy volunteers and aHUS patients. Our results suggested that although *FH1* mutations relates to the development of Japanese aHUS in accordance with other ethnic studies, other factor may be required for factor H polymorphism to be a risk factor of Japanese aHUS.

1. Introduction

Hemolytic uremic syndrome (HUS) is a microvasculature disorder characterized by the triad of microangiopathic hemolytic anemia, renal failure, and thrombocytopenia, and is mainly caused by the enterocolitis with Shiga toxin-producing *Eschericia coli* of the serotype O157:H7 (Karmali et al., 1983, 1985). This form, known as typical HUS, has a good prognosis, and not often affects family members (Kaplan et al., 1998; Ault, 2000; Sánchez-Corral & Melgosa, 2010). In contrast, atypical HUS (aHUS), characterized by the absence of any infection (e.g., Shiga toxin-producing *E. coli, Shigella dysenteriae,* and *Streptococcus pneumoniae*) and its associated-diarrhea, tends to relapse and have a poor prognosis (Kaplan et al., 1998; Ault, 2000; Sánchez-Corral & Melgosa, 2010), and has been classified as either sporadic or familial (Kaplan et al., 1975). Approximately 50% of patients with aHUS have mutations in the genes encoding complement regulatory proteins [e.g., factor H, membrane cofactor protein (MCP or CD46), factor I, factor B, thrombomodulin, and C3] (Atkinson et al., 2005; Caprioli et al., 2006; Delvaeye et al., 2009). In particular, the gene coding factor H, *FH1*, is known to be the most frequently affected in the development of aHUS (Caprioli et al., 2006).

Factor H, a 150-kDa plasma glycoprotein predominantly produced in the liver, consists of 20 homologous units of about 60 amino acid residues each, known as short consensus repeats (SCRs) or the complement control protein units (Ault, 2000). Factor H plays a critical role in the regulation of the alternative complement activation pathway; i.e., this complement component is a cofactor for serine protease factor I in cleaving C3b to its inactive form (C3bi) and accelerates decay of the alternative complement pathway C3bBb convertase complex (Weiler et al., 1976; Whaley and Ruddy, 1976; Pangburn et al., 1977). Several reports demonstrated that anomalous function of factor H, attributed to the mutations in *FH1*, affects the complementary activation and the pathogenesis of aHUS (Pangburn, 2002; Sánchez-Corral et al., 2004; Ferreira and Pangburn, 2007). Actually, Saunders et al. (2006) previously demonstrated that the majority of *FH1* mutations in patients with aHUS causes either single amino acid exchange or premature translation interruption within SCR 20, a domain which contains recognition sites for cell surface ligands, and consequently the

* Corresponding author at: Department of Medicine, Molecular Clinical Pathology, Graduate School of Comprehensive Human Sciences, University of Tsukuba, 1-1-1 Tennoudai, Tsukuba, 305-8575, Japan, Tel.: +81 29 853 3456; fax: +81 29 853 3456.
E-mail address: yamauchi@md.tsukuba.ac.jp (K. Yamauchi).

0161-5890/$ – see front matter © 2011 Elsevier Ltd. All rights reserved.
doi:10.1016/j.molimm.2011.07.017

binding avidity of factor H (to C3b, heparin, or endothelial cells) is reduced.

To date, several linkage analyses have revealed that *FH1* is a candidate gene for aHUS, because its mutations or polymorphisms could be frequently detectable in aHUS patients (Caprioli et al., 2001, 2003; Richards et al., 2001; Neumann et al., 2003; Esparza-Gordillo et al., 2005). However, to our knowledge, the frequency of *FH1* mutations and polymorphisms and their relation to aHUS in Japanese subjects have not been well-defined.

We designed this study with an aim to characterize factor H and its impact on the clinical phenotype in Japanese aHUS patients. Further, we analyzed the frequency of *FH1* mutations and polymorphisms in Japanese patients with aHUS, their family members, and healthy volunteers to clarify its relevance to the pathogenesis of aHUS.

2. Materials and methods

2.1. Subjects

DNA samples were extracted from whole peripheral blood leukocytes obtained from aHUS patients [$n = 10$, 3 men and 7 women; age range 1–40 years (mean ± SE, 19 ± 5 years)], the family members (for the pedigree analysis), and healthy volunteers [$n = 15$, 3 men and 12 women; age range 26–58 years (mean ± SE, 41 ± 3 years)] using QIAamp DNA Blood Mini Kit (Qiagen, Valencia, CA) according to the manufacturer's instructions. We also used 32 healthy volunteer's sera for hemolytic assay. As described previously (Scheiring et al., 2010), aHUS was clinically defined as non-diarrheal and non-Shiga toxin HUS. This study was approved by the ethics committee of Shinshu University, Japan (approval No., 221). All subjects gave their informed consent before participation.

2.2. Serum C3

The C3 concentrations in the serum were measured by turbidimetric immunoassay method (Nittobo, Tokyo, Japan) using a BioMajesty JCA-BM 1650 (JEOL, Tokyo, Japan).

2.3. Quantification of factor H concentration

The factor H concentrations in the serum were measured by the ELISA method as described previously (Oppermann et al., 1990). Briefly, commercial polystyrene immunoplates (Nunc, Roskilde, Denmark) were coated with anti-human factor H (ANTIBODYSHOP, Gentofte, Denmark) in 50 mmol/L sodium bicarbonate, pH 10.6 (1.0 mg protein/L) for 24 h at 4 °C. Plates were washed three times with PBS containing 0.5 g/L Tween 20 (PBS-Tween) after each of the subsequent incubation steps. Unoccupied sites were blocked with the blocking buffer (NOF Corp., Tokyo, Japan) for 30 min at room temperature. The prepared calibrators and samples were then added at 100 μL/well and incubated for 2 h at room temperature. Biotinylated anti-factor H (ANTIBODYSHOP, Gentofte, Denmark) was added at 100 μL/well and incubated for 1 h at room temperature. Horseradish peroxidase-conjugated streptoavidin (Dako, Glostrup, Denmark), diluted 1000-fold with PBS-Tween, was then added at 100 μL/well and incubated for 1 h at room temperature. After final washings, the color reaction was developed with 100 μL/well of 5 g/L t-methylbenzidine dihydrochloride and hydrogen peroxide. After 30-min incubation at room temperature, the reaction was stopped by adding 50 μL of 0.4 mol/L sulfuric acid, and the absorbance at 450 nm was measured using Personal LAB (Biochem ImmunoSystems, PA). A calibration curve was generated, and the factor H concentration in serum was calculated from the curve. Each assay was carried out at lest in duplicate.

2.4. Hemolytic assay

A hemolytic assay was carried out as described previously (Pangburn, 2002) with a small modification. Briefly, sheep erythrocytes were suspended in HEPES buffer (20 mM HEPES, 7 mM $MgCl_2$, 10 mM EGTA, 144 mM NaCl, 1% BSA; pH 7.4) to give a final concentration of 5×10^4 cells/μL. One hundred microliters of the above suspension was mixed with equal volume of serial dilution series of each serum (5, 10, 20, 30, 40, and 50% serum concentration) or saline as a blank, and the mixture was immediately incubated at 37 °C for 30 min. After the mixture was centrifuged at 3500 rpm for 3 min at room temperature, absorbance at 414 nm (A_{414}) of the isolated supernatant was determined using SpectraMax PLUS384 (Molecular Devices Inc., Sunnyvale, CA). The percent hemolytic activity of each sample was determined by subtracting the A_{414} of blank, and dividing by the A_{414} of the control of total lysis (100 μL of serum, 1 μL of 5×10^6 cells/μL sheep erythrocytes suspension and 99 μL of ammonium chloride solution).

2.5. Screening for factor H antibody

The factor H antibodies in the serum were identified by the ELISA method as described previously (Dragon-Durey et al., 2005) with a small modification. Briefly, commercial polystyrene immunoplates were coated with human factor H (Calbiochem, Meudon, France) in PBS (0.3 μg/well) for 24 h at 4 °C. Plates were washed three times after each of the subsequent incubation steps, and blocked unoccupied sites with PBS containing 10 g/L BSA for 1 h at room temperature. The samples were added at at 100 μL/well diluted 1:10 for 1 h at room temperature. Horseradish peroxidase-conjugated goat anti-human IgG solution (Denka-Seiken, Tokyo, Japan) was then added at 100 μL/well and incubated for 1 h at room temperature. After final washings, the color reaction was developed using t-methylbenzidine dihydrochloride and hydrogen peroxide. After 30-min incubation at room temperature, the reaction was stopped by adding 100 μL of 0.3 mol/L sulfuric acid, and the absorbance at 450 nm was measured using Personal LAB. Absorbance above the mean + 2SD of those determined by making measurements of 37 healthy volunteers' sera was considered as positive.

2.6. Screening of FH1 mutations and polymorphisms

FH1 exons were identically amplified by conventional PCR method. The primers used in present study are listed in Table 1. We designed 3 specific primer sets which amplify exons 22 and 23, including C3645T mutation (Ser1191Leu in SCR20) and G3717A mutation (Arg1215Gln in SCR20), and 6 specific primer sets used for recognizing polymorphisms [(C-257T in promoter region, C994A in exon 7 (Ala307Ala in SCR5), G1492A in exon 9 (Ala473Ala in SCR8), A2089G in exon 14 (Gln672Gln in SCR11), G2881T in exon 19 (Glu936Asp in SCR16), and G3364A in exon 20 (Thr1097Thr in SCR18)] according to previous study (Caprioli et al., 2003). PCR was performed on a Gene Amp PCR system 9700 (Applied Biosystems, Foster City, CA). After the purification of PCR products, direct DNA sequencing was performed using a BigDye™ Terminator Cycle Sequencing Ready Reaction Kit and an ABI Prism 3100 Genetic Analyzer (both from Applied Biosystems).

2.7. Statistical methods

All experiments were performed at least three times. Data are presented as mean ± 2SD. Statistical analysis was performed by non-paired t test and chi-square test depending on the data set concerned. A p value of less than 0.05 was accepted as statistically significant.

Table 1
Primers set for factor H gene (FH1) screening.

Region	SCR	Foward	Reverse
Promoter	–	5′-CAAGCACTGCATTCTTGGCA-3′	5′-GCTAGGGAAATTCTCCGTTG-3′
exon 7	SCR 5	5′-TTTAACGGATACTTATTTCTGCATTATCC-3′	5′-TTCAGAATTAAGAAATGGGTCAAGATATG-3′
exon 9	SCR 8	5′-ATAGATATTGAATGGGTTTATTTCTGAA-3′	5′-GTTGAGCTGACCATCCATCTTTC-3′
exon 14	SCR 11	5′-TATATTGTAAAACAGACAATTTAACC-3′	5′-ATACAAAATACAAAAGTTTTGACAAG-3′
exon 19	SCR 16	5′-GATGTCATAGTAGCTCCTGTATTGTTTATTT-3′	5′-CCACTTACACTTTGAATGAAGAATATTTATC-3′
exon 20	SCR 18	5′-CACTTCTTTTTTTTCTATTCAGACACC-3′	5′-AGAATTGAATTTTAAGCACCATCAG-3′
exon 22	SCR 19	5′-TGAAATATCAGACTCATCACAGA-3′	5′-ATACAGTGCTGTGTTTGCG-3′
exon 23	SCR20[a]	5′-GTTCTGAATAAAGGTGTGCAC-3′	5′-GCCAAACAGAAGCTTTATTC-3′
exon 23	SCR20[b]	5′-CCCCGTTACACACAAATTCAA-3′	5′-CTACATAGTTGGTTTGGAT-3′

[a] Upstream region of exon 23.
[b] Downstream region of exon 23.

3. Results

3.1. Clinical features of patients with aHUS

Clinical features and genetic findings of *FH1* of 10 patients with aHUS were summarized in Tables 2 and 3, respectively.

Patient 1 (A-6). We analyzed for factor H status using patient's serum, obtained after 1-yr from the episode. Serum factor H level was also significantly decreased (75% of healthy volunteer's serum, $p < 0.01$). The heterozygous G3717A mutation, and heterozygous polymorphisms of C-257T, A2089G, G2881T, and G1492A were found in FH1. Anti-factor H antibody was not detected. Other complement regulatory factors were normal (i.e., factor I level was 14.5 mg/dl, and expression of MCP on lymphocytes was not decreased). The ADAMTS13 activity was normal.

Patient 2 (B-11). We analyzed for factor H status using patient's serum, obtained after 3-yrs from the first episode. Factor H level was slightly increased (114% of healthy volunteer's serum, $p < 0.01$). The heterozygous G3717A mutation, and five heterozygous disease risk polymorphisms (C-257T, A2089G, G2881T, C994A, G1492A,

Table 2
Clinical features of aHUS patients.

Case (Pedigree No)	Age	Gender	Onset age	Clinical findings and evolutions
1 (A-6)	1 yr	F	4 mo	Renal insufficiency and hypocomplementemia. Under treatment (plasmapheresis and FFP administration).
2 (B-11)	34 yr	M	31 yr	Renal insufficiency, hemolytic anemia, biliruminemia, hypocomplementemia, and thrombocytopenia. Under treatment (Chronic hemodialysis and plasmapheresis).
3 (B-12)	38 yr	F	31 yr	Hypocomplementemia. Under treatment (Chronic hemodialysis).
4 (C-6)	29 yr	F	6 mo	Hemolytic anemia, and thrombocytopenia. Recurrence of aHUS after pregnancy and partum. Remission after PSL administration and steroid pulse therapy.
5 (D-3)	17 yr	F	13 yr	Renal insufficiency, hemolytic anemia, bilirubinemia, and thrombocytopenia. Remission after continuous hemodialysis.
6	4 yr	F	n.c.	Renal insufficiency, hemolytic anemia, and thrombocytopenia. Under treatment (plasmapheresis).
7	8 yr	M	4 yr	Renal insufficiency, hemolytic anemia, bilirubinemia, thrombocytopenia and hypocomplementemia. Recurrence of aHUS after infection of influenzavirus B. Under supportive treatment.
8	40 yr	M	40 yr	Renal insufficiency, and hemolytic anemia. Under treatment (hemodialysis, plasmapheresis, PSL administration, and steroid pulse therapy).
9	7 yr	F	7 mo	Severe thrombocytopenia. Recurrence. Before treatment.
10	9 yr	F	n.c.	Renal insufficiency, hemolytic anemia, thrombocytopenia, and hypocomplementemia. Before treatment.

FFP, fresh frozen plasama; PSL, prednisolone; n.c., not clear.

Table 3
Factor H status in Japanese Ahus.

Case (pedigree no.)	Polymorphisms						Mutation	Serum factor H levels	Hemolytic activity[b]	Anti-factor H antibody
	C-257T	C994A	G1492A	A2089G	G2881T	G3364A	G3717A	(relative to normal value %)[a]		
1 (A-6)	CT	CC	GA	AG	GT	GG	AG	75*	+	–
2 (B-11)	CT	CA	GA	AG	GT	GG	AG	114*	–	–
3 (B-12)	CC	CA	GA	AA	GG	GG	AG	131*	+	–
4 (C-6)	CC	CC	AA	AA	GG	GG	GG	74*	–	–
5 (D-3)	CC	CC	AA	AA	GG	GG	GG	n.t.	–	–
6	CC	CC	AA	AA	GG	GG	GG	62*	+	+
7	CT	CA	n.d.	AA	GG	GA	GG	108	+	–
8	TT	CC	GA	GG	TT	GG	GG	143*	+	–
9	TT	CC	GG	GG	TT	GA	GG	125*	–	–
10	TT	CC	GG	GG	TT	GA	GG	80*	–	+

[a] Serum factor H levels were expressed as the relative to normal value (1388 ± 547 mg/L), determined by making measurements of healthy volunteers' sera.
[b] The percent hemolytic activity of each patient's serum was compared with those of normal value, determined by making measurements of 32 healthy volunteers' sera as described in Section 2. The subjects with a significantly high level of hemolytic activity were expressed as "positive". n.d., not determined. n.t., not tested.
* $p < 0.01$ vs normal value.